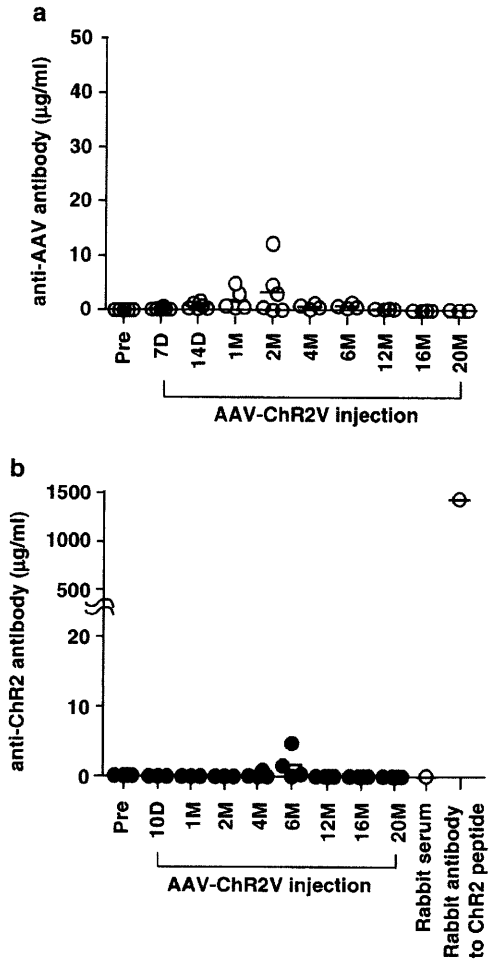

Figure 7 Humoral immune responses to the viral vector and transgene. Production levels of the antibodies to the AAV2 vector (**a**) and the therapeutic gene, ChR2 (**b**), were studied in RCS rats following a single intra-vitreous injection of rAAV-ChR2V. The time after injection is indicated. The antibody levels against both AAV2 and ChR2 were quite low compared with the antibody levels in serum of an immunized rabbit, which were considered as the effective dose to react with antigens.

month after the rAAV-ChR2V injection was higher than that before the injection. These data suggested that a change in the inflammation status occurred from 1 week to 1 month after rAAV administration. After this period, the ratios decreased to the pre-injection value and were stable for 1 year. To assess the inflammation status, we studied T regulatory cells. As shown in Figure 8b, a significant increase in the number of $CD4^+CD25^+$ cells was observed at 1 week after the rAAV-Venus and rAAV-ChR2V injections compared with the numbers before the injections. There was no significant difference in the inflammation status between the rAAV injections. As a positive control of inflammation, EIU also increased the population of $CD4^+CD25^+$ cells, which is consistent with a report by Toda *et al.*[19]

DISCUSSION

The results of this study demonstrate that the strategy of restoration of vision and light responses in photoreceptor-degenerated RCS (*rdy/rdy*) rats by rAAV-ChR2V administration was technically feasible and safe. Most importantly, ChR2 function, which was confirmed by measuring VEPs, was not reduced over the whole observation period after rAAV-ChR2V administration (Figure 1). A single administration of rAAV-ChR2V restored the light sensitivity over the lifespan of the rat model.

The eye is considered to be an immunologically protected space.[20] This immune privilege is the result of multiple layers and mechanisms, including the blood–retina barrier and other physical barriers, such as the immunosuppressive microenvironment against deviant systemic immunity, that limit the production of pro-inflammatory effector cells. We predicted that systemic dissemination of a virus would be limited by these immune systems after intra-vitreous injection. To investigate the systemic dissemination of rAAV, ribonucleic acids were isolated from each organ and the expressions of the Venus protein, which was fused to rAAV-ChR2, were studied (Figure 2). Venus expression was notable in the retina. Contrary to our expectations, the expression was also detected in the intestine, lung and heart in some cases. The RCS (*rdy/rdy*) animal model, which genetically causes loss of photoreceptors, is reported to have some breakdown of the blood–retina barrier or other mechanisms.[21–24] Therefore, the rAAV vector might have been disseminated to the other organs. Supporting this hypothesis, the efficiency of rAAV-derived gene transfer was higher in RCS rats than in normal rats (data not shown). This result suggests that some breakdown of the retinal barriers increased the permeability to rAAV.

The genomes transferred by rAAV tend to persist in cells mainly in an episomal, non-integrated form.[25] The transferred genomes in episomal form are diluted by cell division. However, when rAAV-carried genomes are inserted into chromosomes of cells with high proliferation ability, the genomes are preserved. There were some differences in gene delivery by rAAV among the samples obtained from the intestine, lung and heart. These differences might be the result of differences in the insertion forms of the rAAV genomes.

In gene therapy, tumour formation caused by the insertion of a transgene into the genome has been reported.[12–14] We did not observe tumour formation in any of the rats that received the rAAV injections (data not shown). For more information regarding tumour formation, further studies are needed by using methods such as Northern blotting, integration site analysis[26] and oncogene analysis.

We also investigated the inflammatory responses caused by the gene transfer by using the EIU model as a positive control of inflammation. EIU caused ocular inflammation, including leucocyte infiltration into the vitreous humour (Figure 4d) and leucocyte adhesion to the retinal vessels (Figures 6c and d). These findings are consistent with those of previous reports.[15,27] However, we did not observe such inflammatory cells in the retinas treated with rAAV-Venus or rAAV-ChR2V. Therefore, rAAV-ChR2V administration did not induce inflammation arising from bacterial infection.

GFAP is reportedly expressed because of gliosis and hypertrophy of macroglial cells.[28] Moreover, GFAP is expressed in astrocytes in the retina usually, but in Müller cells under pathological or stress conditions.[29] GFAP was also reported to be upregulated in the brain astrocytes during the inflammatory response.[30] Beurel and Jope[31] revealed that GFAP upregulation is caused by the production of the inflammatory cytokine interleukin-6. The absence of GFAP upregulation by viral injection (Figures 5b–d) demonstrates the lack of glial activation derived from inflammation. Our study showed that GFAP was expressed throughout the retina in the untreated RCS rats and that the expression was decreased and restricted by the rAAV-ChR2V injection (Figure 5c). These results reveal that activation of RGCs by ChR2 may have a protective effect on the inner retina.[32,33] NF-κB expression in the retina was restricted to the ganglion cell layers in all

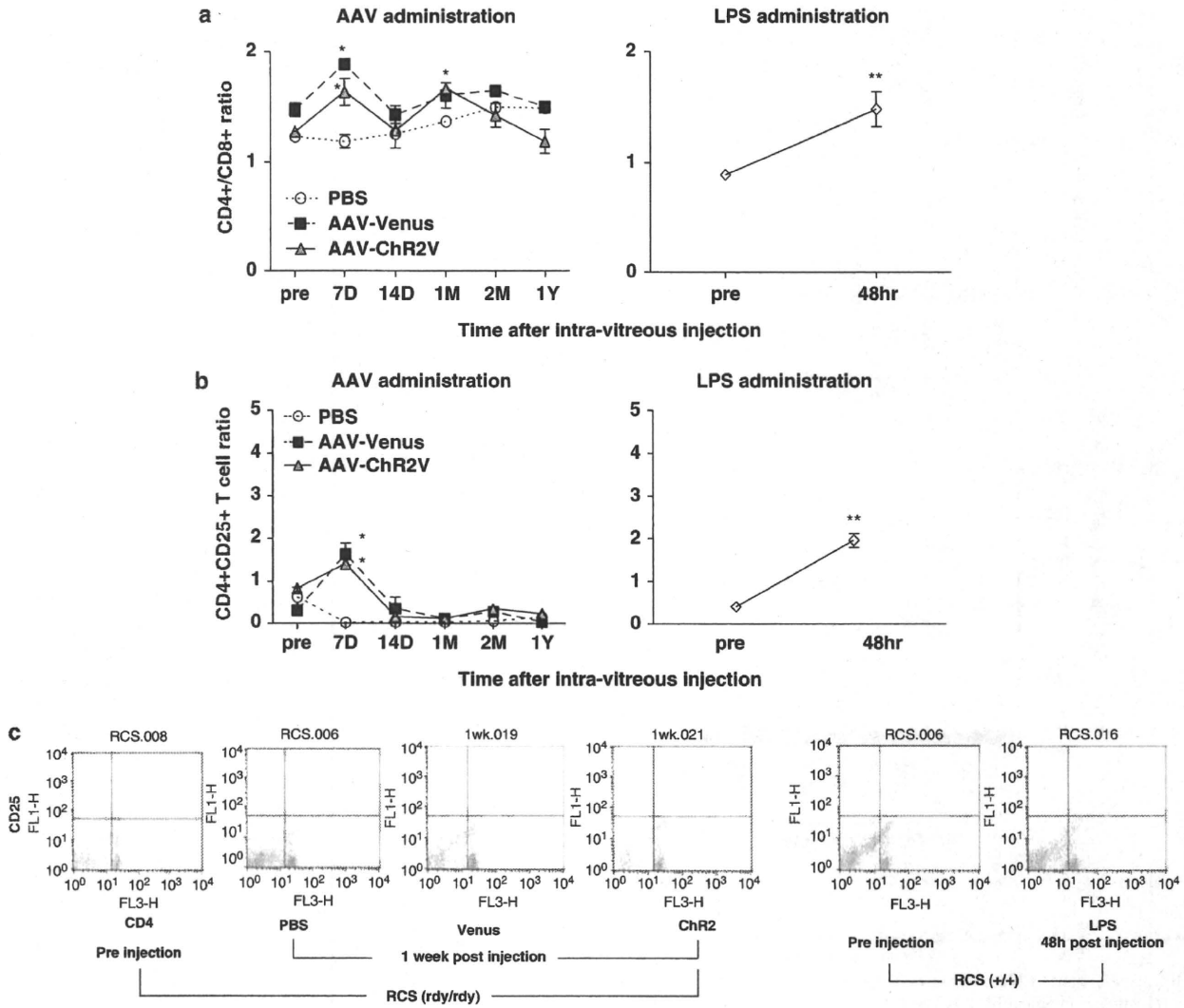

Figure 8 T-cell ratio in the peripheral blood. Lymphocytes were isolated from the peripheral blood before and after injection of PBS, rAAV-Venus or rAAV-ChR2V. The lymphocytes were incubated with anti-T-cell receptor-associated CD3, anti-CD4 and anti-CD8a mAbs, and analysed by flow cytometry. The blood of lipopolysaccharide-administrated rats as a positive control of inflammation was also analysed. The T-cell ratio of $CD4^+/CD8^+$ (**a**) and $CD4^+CD25^+$ (T regulatory cells) (**b**) was calculated. (**c**) Representative data of T regulatory analysis are indicated. All data are represented as the mean (s.d.) of four to seven animals.

the experiments and there was no staining of the other inner retinal cells, which was caused by stress.[34] We also demonstrated the potent expression of NF-κB p65 in the rAAV-ChR2V-injected retinas. These results are consistent with reports that constitutive NF-κB activity is the result of ongoing synaptic activity.[35,36]

The T-lymphocyte analysis demonstrated that the $CD4^+/CD8^+$ ratio was higher in all the rAAV-treated rats at 1 week after the injection than before the injection, and in the rAAV-ChR2V-treated rats, the ratio was high at 1 month after injection (Figure 8a). However, these increases were transient and returned to the pre-injection level. This expansion allows cross-talk between different types of cells in the ongoing immune response.[17] Kim and Lim[18] reported that $CD4^+/CD8^+$ expansion is caused by bacterial infection. After 1 week, the ratio increased in all the rAAV-injected rats. Thus, there might have been some immune reactions such as antigen presentation to rAAV. At 1 month after the rAAV-ChR2V injection, the ratio increased again. As shown in Figure 1, the maximum ChR2 function was recorded at 1 month in the visual cortex first. Thus, some immune reactions might have been induced by increased ChR2 expression but were well tolerated at 2 months after the injection.

Currently, the best characterized regulatory cells are $CD4^+CD25^+$ T cells.[37] These cells can suppress host immune responses and modulate the immune responses in autoimmune diseases, allergy, transplantation and infectious diseases.[38,39] CD25, an interleukin-2 receptor, is reported to be an inflammation marker on $CD4^+$ lymphocytes.[18] In the EIU experiment, we observed expansion of $CD4^+CD25^+$ cells, which is consistent with the report by Toda *et al.*[19] A significant increase in the number of $CD4^+CD25^+$ cells was observed in both the rAAV-Venus and the rAAV-ChR2V rats at 1 week after the injections compared with the pre-injection values (Figure 8b), although there was no significant difference in the results between the rAAV-Venus and the rAAV-ChR2V injections.

These results demonstrate that the inflammation-like immunological reaction was caused by AAV and not by ChR2.

To assess the possibility of a systemic humoral immune response to the viral vector or transgene product, we measured the antibody levels of the rAAV2 capsid and ChR2 in serum by enzyme-linked immunosorbent assay. Intra-vitreous injection caused relatively little antibody production (Figure 7a) compared with the different route of AAV injection used by Zhang *et al.*[16] Li *et al.*[40] demonstrated that a single intra-vitreous injection of AAV2 causes increased AAV antibody production at 2 months after injection. Our data are consistent with their report in terms of the timing of increase and the amount of antibody production (Figure 7a). We anticipated that ChR2 expression would cause antibody production because ChR2 is not inherent to humans. However, the production levels were relatively low (Figure 7b) and were insufficient to induce a humoral immune response.

In conclusion, an immune reaction can be caused by AAV administration and ChR2 protein expression, but will be well tolerated. It should be noted that the experiments were performed in rats and cannot be directly extrapolated to humans, who constitute a far more immunologically heterogeneous population. However, these findings will help studies of ChR2 gene transfer to restore vision in progressed RP.

MATERIALS AND METHODS

Animals

In total, 59 (6-month-old male) RCS rats (43 dystrophic (*rdy/rdy*)); 16 non-dystrophic (+/+) were used in this study (Table 1). The animals were maintained and used in accordance with the ARVO Statement for the *Use of Animals in Ophthalmic and Vision Research and the Guidelines for Animal Experiments of Tohoku University.* All the animal experiments were conducted with the approval of the Animal Research Committee, School of Medicine, Tohoku University. To compare the functions, the control and treated rats were age-matched in each experiment.

Induction of EIU

As a model of ocular inflammation,[41] RCS (+/+) rats received a single intra-vitreous injection of 5 μg lipopolysaccharide from *Escherichia coli* (055:B5; Sigma, St Louis, MO, USA) in 5 μl phosphate-buffered saline (PBS) to cause EIU. After 48 h of lipopolysaccharide administration, the inflammation status was studied.

Preparation of AAV vector carrying the ChR2 gene construct

The *N*-terminal fragment (residues 1–315) of ChR2 (GenBank accession no. AF461397) was fused to a fluorescent protein, Venus, in frame at the end of the ChR2-coding fragment described previously.[5] The ChR2V or Venus gene was introduced into the *Eco*RI and *Hin*dIII sites of the 6P1 plasmid.[42] The synapsin promoter was exchanged for a hybrid cytomegalovirus enhancer/chicken β-actin promoter,[42] and AAV-ChR2V and AAV-Venus were constructed. The pAAV-RC and p-Helper plasmids were obtained from Stratagene (La Jolla, CA, USA). Semi-confluent 293T cells on 15-cm plates were co-transfected with split-packaging plasmids—AAV-ChR2V (or AAV-Venus), pAAV-RC and p-Helper—by using a calcium phosphate-based protocol according to the manufacturer's instructions (Agilent Technologies, La Jolla, CA, USA). The rAAV vectors (rAAV-ChR2V, rAAV-Venus) were purified by using the method of Auricchio *et al.*[43–45]

rAAV vector injection

The rAAV-ChR2V or rAAV-Venus vector was administered by intra-vitreous injection into the left eye of 6-month-old RCS (*rdy/rdy*) rats. In brief, the rats were anaesthetised by intramuscular injection of a mixture of ketamine (66 mg ml^{-1}) and xylazine (33 mg kg^{-1}). Under an operating microscope, the conjunctiva was incised to expose the sclera. A total volume of 5 μl of vector suspension at a concentration of 5×10^{12} genomic particles per μl was administered by intra-vitreous injection through the ora serrata with a 10-μl Hamilton syringe and a 32-gauge needle (Hamilton Company, Reno, NV, USA).

Recording of VEPs

VEPs were recorded by using Neuropack MEB-9102 (Nihon Kohden, Tokyo, Japan). The method of recording was derived from a combination of protocols used by Papathanasiou *et al.*[46] and Iwamura *et al.*[47] In brief, at least 7 days before the experiments, recording electrodes (silver–silver chloride) were placed epidurally on each side 7 mm behind the bregma and 3 mm lateral to the midline, and a reference electrode was placed epidurally on the midline 12 mm behind the bregma. Under ketamine–xylazine anaesthesia, the pupils were dilated with 1% atropine and 2.5% phenylephrine hydrochloride. The ground electrode clip was placed on the tail. Photic stimuli of 20-ms duration were applied at a frequency of 0.5 Hz and generated by pulse activation of a blue light-emitting diode with light-emitting wavelengths in the range 435–500 nm (peak, 470 nm). A total of 100 consecutive response waveforms were averaged for the VEP measurements.

Table 1 The Number of samples examined in this study

	VEP	*PCR*	*Expression in retina (whole mount)*	*Histology (HE)*	*Immuno-histochemistry*	*Leukocyte adhesion*	*Antibody detection*	*Flow cytometry*	*Total (n)*
No treatment (+/+)				3	3	3			9
Pre-treatment (+/+)								7	7
LPS administration (+/+)				3		4		7	
No treatment (*rdy/rdy*)				3	3	3			9
Pre-injection for PBS (*rdy/rdy*)								4	4
After PBS injection (*rdy/rdy*)								4	
Pre-injection for rAAV-Venus (*rdy/rdy*)								4	10
After rAAV-Venus injection (*rdy/rdy*)			3		3			4	
Pre-injection for rAAV-ChR2V (*rdy/rdy*)	20						3–6	4	20
After rAAV-ChR2V injection (*rdy/rdy*)	20	4	3	3	3	3	3–6	4	

Abbreviations: ChR2V, channelrhodopsin-2 fused to Venus; HE, hematoxylin and eosin; LPS, lipopolysaccharide; PBS, phosphate-buffered saline; PCR, polymerase chain reaction; rAAV, adeno-associated virus type 2; VEP, visually evoked potential.

Ribonucleic acid isolation and rAAV-derived protein detection by RT-PCR analysis

Total ribonucleic acids were extracted (TRIreagent; Sigma) from the retina, brain, lung, testis, liver, kidney, intestine, lung and heart. cDNA was synthesised (First-Strand cDNA synthesis kit; GE Healthcare, Piscataway, NJ, USA) and the tracer fusion protein, Venus, expression was investigated by using a semi-quantitative RT-PCR method. As the individual internal control, we performed PCR with β-actin. The primer sequences were as follows: 5′-TCATGAAGTGT GACGTTGACATCCGT-3′ (sense) and 5′-CCTAGAAGCATTTGCGGTGCAC GATG-3′ (antisense) for β-actin; 5′-GACGTAAACGGCCACAAGTT-3′ (sense) and 5′-GAACTCCAGCAGGACCATGT-3′ (antisense) for Venus. Following electrophoresis on 1.0% agarose gel, DNA was detected by staining with GelRed (Biotium, Inc., Hayward, CA, USA).

Histology

After death, the eyeballs were enucleated, immersed in 4% paraformaldehyde in PBS overnight at 4 °C and embedded in paraffin. Serial sections (4 μm) of whole eyes were cut sagittally, through the cornea and parallel to the optic nerve, and stained with haematoxylin and eosin. Microscopic examination of the sections was then performed (AxioImager A1; Carl Zeiss, Tokyo, Japan).

The ChR2V expression profile in the retina was studied according to the method we previously described.[5] In brief, the eyes were fixed and the retinas were flat-mounted on slides. Venus fluorescence was visualised under a fluorescence microscope (BZ-9000; Keyence Corp., Osaka, Japan).

Immunohistochemistry

Rat eyes were fixed overnight at 4 °C in 4% paraformaldehyde in PBS (pH 7.4). The retinas were rinsed with PBS and immersed in 10, 20 and 30% sucrose in PBS at 4 °C. Samples were embedded in optimal cutting temperature compound (Sakura, Tokyo, Japan) under liquid nitrogen and stored at −80 °C. Cryosections (10 μm) of tissue were mounted on slides and air dried. Then, retinal sections were washed with PBS and treated for 15 min with 0.3% H_2O_2 in methanol. After washing with PBS, the sections were incubated with mouse anti-rat NF-κB p65 (C-20) antibody (1:200; Santa Cruz Biotechnology, Santa Cruz, CA, USA) and mouse anti-rat GFAP antibody (1:250; Nihon Millipore, Tokyo, Japan) in antibody diluent buffer (0.05% Tween-20, 3% bovine serum albumin and 3% goat serum in PBS) overnight at 4 °C. After washing with 0.05% Tween-20 in PBS, the sections were incubated with horseradish peroxidase-conjugated goat anti-mus immunoglobulin G as the secondary antibody for 1 h at room temperature. After washing with TBST (150 mM NaCl, 0.1% Tween-20 in 20 mM Tris-HCl), the immunohistochemical reactions were visualised by using an Envision DAB kit (Dako, Tokyo, Japan). The sections were counterstained with haematoxylin. As a negative control for staining, the first antibodies were replaced with non-immune mouse immunoglobulin G (Dako). The sections were observed under a microscope (AxioImager A1; Carl Zeiss).

Lectin labelling of the retinal vasculature and adherent leucocytes

Leucocytes adhering to the retinal vasculature were imaged by perfusion labelling with fluorescein isothiocyanate-coupled concanavalin A lectin (Vector Laboratories, Burlingame, CA, USA).[27] After deep anaesthesia, the chest cavity was opened, a 20-gauge perfusion cannula was introduced into the aorta and a part of the liver was excised. After injection of 20 ml PBS to remove erythrocytes and non-adherent leucocytes, 20 ml of fluorescein isothiocyanate-conjugated concanavalin A lectin (40 μg ml^{-1}) was injected. Residual unbound concanavalin A was removed with PBS perfusion. After the eyeballs were enucleated, the retina was flat-mounted and imaged under a fluorescence microscope (Axiovert 40; Carl Zeiss).

Enzyme-linked immunosorbent assay

To detect serum antibodies to the rAAV2 capsid and the transgenic protein, ChR2, we coated enhanced protein-binding enzyme-linked immunosorbent assay plates with 10^9 viral particles per well of rAAV2 in 100 μl of 0.1 M sodium carbonate buffer (pH 9.6) and with 0.2 μg per well peptide coding for ChR2 by using a peptide coating kit (TaKaRa, Shiga, Japan) at 4 °C overnight. The wells were blocked with 10% fetal bovine serum-0.1% Tween in PBS for 30 min at 37 °C. Then, serum dilutions were added and incubated for 4 °C overnight. Dilutions of a rabbit anti-AAV2 capsid protein (American Research Product, Belmont, MA, USA) and a rabbit anti-ChR2 protein (TaKaRa) served as positive controls. The plates were incubated with horseradish peroxidase-conjugated anti-rabbit immunoglobulin G or anti-rat immunoglobulin G at 37 °C for 1 h in the presence of 3% goat serum. The reactions were visualised by adding one-step tetramethylbenzidine substrate (Promega, Tokyo, Japan). The reactions were stopped by adding 1 N HCl and read at 450 nm with a VERS Amax plate reader (Molecular Devices, Osaka, Japan). Each value was determined in triplicate.

Analysis of T lymphocytes

Peripheral blood $CD4^+$ cells have a central role in regulating the cell-mediated immune response to infection. Often known as helper T cells, they act on other cells of the immune system to promote various aspects of the immune response, including immunoglobulin isotype switching and affinity maturation and enhanced activity of natural killer cells and cytotoxic T cells. $CD4^+$ cells also act by releasing cytokines in response to antigenic stimulation. One of the major roles of $CD4^+$ cells is the activation of macrophages. During the course of hepatitis C virus infection, two different immunological statuses can be observed. In the acute phase of infection, $CD4^+$ helper T cells contribute to the induction and maintenance of a functional $CD8^+$ cell response. In the chronic phase, T regulatory ($CD4^+CD25^+$) cells suppress $CD8^+$ cell responses, and thereby help the virus to persist.[48] It is important to calculate these ratios to observe the immunological status.

Before and after the rAAV injection, peripheral blood was collected from the tail vein. Lymphocytes were isolated with PharmLyse (BD Bioscience, San Jose, CA, USA). After isolation, a mixture of monoclonal antibodies (mAbs) specific for CD3 (conjugated with Alexa Fluor 647; AbD Serotec, Oxford, UK), CD4 (conjugated with PE-Cy5; BD Bioscience), CD8a (conjugated with R-PE; BD Bioscience) and CD25 (conjugated with fluorescein isothiocyanate; BD Bioscience) was added to the cells, which were then incubated at 4 °C overnight. Flow-cytometric analysis was performed by using FACS Calibur (BD Bioscience) after washing the cells with PBS. For gating and calculation, CellQuest software (BD Bioscience) was used. In the FACS analysis, 10 000 cells were examined for each sample.

Statistical analysis

Statistical analysis was performed by using GraphPad Prism (GraphPad Software, San Diego, CA, USA). The criterion for statistical significance was $P<0.05$ by Dunnett multiple comparison test.

CONFLICT OF INTEREST

The authors declare no conflict of interest.

ACKNOWLEDGEMENTS

This work was partly supported by Grants-in-Aid for Scientific Research from the Ministry of Education, Culture, Sports, Science and Technology of Japan (nos. 21791664 and 21200022); Science and Culture and Special Coordination Funds for Promoting Science and Technology of the Japanese Government, Strategic Research Programme for Brain Sciences (SRPBS); the Ministry of Health, Labour and Welfare of Japan; and Japan Foundation for Aging and Health and the Programme for Promotion of Fundamental studies in Health Sciences of the National Institute of Biomedical Innovation (NIBIO). I also thank Teru Hiroi for technical support in animal treatment.

1 Hartong DT, Berson EL, Dryja TP. Retinitis pigmentosa. *Lancet* 2006; **368**: 1795–1809.
2 Santos A, Humayun MS, de Juan Jr E, Greenburg RJ, Marsh MJ, Klock IB *et al.* Preservation of the inner retina in retinitis pigmentosa. A morphometric analysis. *Arch Ophthalmol* 1997; **115**: 511–515.
3 Nagel G, Szellas T, Huhn W, Kateriya S, Adeishvili N, Berthold P *et al.* Channelrhodopsin-2, a directly light-gated cation-selective membrane channel. *Proc Natl Acad Sci USA* 2003; **100**: 13940–13945.

4 Bi A, Cui J, Ma YP, Olshevskaya E, Pu M, Dizhoor AM *et al.* Ectopic expression of a microbial-type rhodopsin restores visual responses in mice with photoreceptor degeneration. *Neuron* 2006; **50**: 23–33.
5 Tomita H, Sugano E, Yawo H, Ishizuka T, Isago H, Narikawa S *et al.* Restoration of visual response in aged dystrophic RCS rats using AAV-mediated channelopsin-2 gene transfer. *Invest Ophthalmol Vis Sci* 2007; **48**: 3821–3826.
6 Lagali PS, Balya D, Awatramani GB, Munch TA, Kim DS, Busskamp V *et al.* Light-activated channels targeted to ON bipolar cells restore visual function in retinal degeneration. *Nat Neurosci* 2008; **11**: 667–675.
7 Tomita H, Sugano E, Isago H, Hiroi T, Wang Z, Ohta E *et al.* Channelrhodopsin-2 gene transduced into retinal ganglion cells restores functional vision in genetically blind rats. *Exp Eye Res* 2010; **90**: 429–436.
8 Ishizuka T, Kakuda M, Araki R, Yawo H. Kinetic evaluation of photosensitivity in genetically engineered neurons expressing green algae light-gated channels. *Neurosci Res* 2006; **54**: 85–94.
9 Wang H, Peca J, Matsuzaki M, Matsuzaki K, Noguchi J, Qiu L *et al.* High-speed mapping of synaptic connectivity using photostimulation in Channelrhodopsin-2 transgenic mice. *Proc Natl Acad Sci USA* 2007; **104**: 8143–8148.
10 Tomita H, Sugano E, Fukazawa Y, Isago H, Sugiyama Y, Hiroi T *et al.* Visual properties of transgenic rats harboring the channelrhodopsin-2 gene regulated by the thy-1.2 promoter. *PLoS One* 2009; **4**: e7679.
11 Monville C, Torres E, Thomas E, Scarpini CG, Muhith J, Lewis J *et al.* HSV vector-delivery of GDNF in a rat model of PD: partial efficacy obscured by vector toxicity. *Brain Res* 2004; **1024**: 1–15.
12 Aiuti A, Bachoud-Lévi AC, Blesch A, Brenner MK, Cattaneo F, Chiocca EA *et al.* Progress and prospects: gene therapy clinical trials (part 2). *Gene Therapy* 2007; **14**: 1555–1563.
13 Alexander BL, Ali RR, Alton EW, Bainbridge JW, Braun S, Cheng SH *et al.* Progress and prospects: gene therapy clinical trials (part 1). *Gene Ther* 2007; **14**: 1439–1447.
14 Thomas CE, Ehrhardt A, Kay MA. Progress and problems with the use of viral vectors for gene therapy. *Nat Rev Genet* 2003; **4**: 346–358.
15 Koizumi K, Poulaki V, Doehmen S, Welsandt G, Radetzky S, Lappas A *et al.* Contribution of TNF-α to leukocyte adhesion, vascular leakage, and apoptotic cell death in endotoxin-induced uveitis *in vivo*. *Invest Ophthalmol Vis Sci* 2003; **44**: 2184–2191.
16 Zhang YC, Powers M, Wasserfall C, Brusko T, Song S, Flotte T *et al.* Immunity to adeno-associated virus serotype 2 delivered transgenes imparted by genetic predisposition to autoimmunity. *Gene Therapy* 2004; **11**: 233–240.
17 Damoiseaux JG, Cautain B, Bernard I, Mas M, van Breda Vriesman PJ, Druet P *et al.* A dominant role for the thymus and MHC genes in determining the peripheral CD4/CD8 T cell ratio in the rat. *J Immunol* 1999; **163**: 2983–2989.
18 Kim SA, Lim SS. T lymphocyte subpopulations and interleukin-2, interferon-γ, and interleukin-4 in rat pulpitis experimentally induced by specific bacteria. *J Endod* 2002; **28**: 202–205.
19 Toda A, Piccirillo CA. Development and function of naturally occurring CD4+CD25+ regulatory T cells. *J Leukoc Biol* 2006; **80**: 458–470.
20 Simpson E. A historical perspective on immunological privilege. *Immunol Rev* 2006; **213**: 12–22.
21 Caldwell RB, McLaughlin BJ. Permeability of retinal pigment epithelial cell junctions in the dystrophic rat retina. *Exp Eye Res* 1983; **36**: 415–427.
22 Caldwell RB, McLaughlin RJ, Boykins LG. Intramembrane changes in retinal pigment epithelial cell junctions of the dystrophic rat retina. *Invest Ophthalmol Vis Sci* 1982; **23**: 305–318.
23 Caldwell RB, Wade LA, McLaughlin BJ. A quantitative study of intramembrane changes during cell junctional breakdown in the dystrophic rat retinal pigment epithelium. *Exp Cell Res* 1984; **150**: 104–117.
24 Chang CW, Defoe DM, Caldwell RB. Retinal pigment epithelial cells from dystrophic rats form normal tight junctions *in vitro*. *Invest Ophthalmol Vis Sci* 1997; **38**: 188–195.
25 Nakai H, Yant SR, Storm TA, Fuess S, Meuse L, Kay MA. Extrachromosomal recombinant adeno-associated virus vector genomes are primarily responsible for stable liver transduction *in vivo*. *J Virol* 2001; **75**: 6969–6976.
26 Niemeyer GP, Herzog RW, Mount J, Arruda VR, Tillson DM, Hathcock J *et al.* Long-term correction of inhibitor-prone hemophilia B dogs treated with liver-directed AAV2-mediated factor IX gene therapy. *Blood* 2009; **113**: 797–806.
27 Satofuka S, Ichihara A, Nagai N, Yamashiro K, Koto T, Shinoda H *et al.* Suppression of ocular inflammation in endotoxin-induced uveitis by inhibiting nonproteolytic activation of prorenin. *Invest Ophthalmol Vis Sci* 2006; **47**: 2686–2692.
28 Reichelt W, Dettmer D, Bruckner G, Brust P, Eberhardt W, Reichenbach A. Potassium as a signal for both proliferation and differentiation of rabbit retinal (Muller) glia growing in cell culture. *Cell Signal* 1989; **1**: 187–194.
29 Hartig W, Grosche J, Distler C, Grimm D, el-Hifnawi E, Reichenbach A. Alterations of Muller (glial) cells in dystrophic retinae of RCS rats. *J Neurocytol* 1995; **24**: 507–517.
30 Hao LY, Hao XQ, Li SH, Li XH. Prenatal exposure to lipopolysaccharide results in cognitive deficits in age-increasing offspring rats. *Neuroscience* 2010; **166**: 763–770.
31 Beurel E, Jope RS. Lipopolysaccharide-induced interleukin-6 production is controlled by glycogen synthase kinase-3 and STAT3 in the brain. *J Neuroinflammation* 2009; **6**: 9.
32 Ni YQ, Gan DK, Xu HD, Xu GZ, Da CD. Neuroprotective effect of transcorneal electrical stimulation on light-induced photoreceptor degeneration. *Exp Neurol* 2009; **219**: 439–452.
33 Morimoto T, Miyoshi T, Sawai H, Fujikado T. Optimal parameters of transcorneal electrical stimulation (TES) to be neuroprotective of axotomized RGCs in adult rats. *Exp Eye Res* 2010; **90**: 285–291.
34 Wang J, Jiang S, Kwong JM, Sanchez RN, Sadun AA, Lam TT. Nuclear factor-kappaB p65 and upregulation of interleukin-6 in retinal ischemia/reperfusion injury in rats. *Brain Res* 2006; **1081**: 211–218.
35 Kaltschmidt C, Kaltschmidt B, Neumann H, Wekerle H, Baeuerle PA. Constitutive NF-kappa B activity in neurons. *Mol Cell Biol* 1994; **14**: 3981–3992.
36 O'Neill LA, Kaltschmidt C. NF-kappa B: a crucial transcription factor for glial and neuronal cell function. *Trends Neurosci* 1997; **20**: 252–258.
37 O'Garra A, Vieira P. Regulatory T cells and mechanisms of immune system control. *Nat Med* 2004; **10**: 801–805.
38 Sakaguchi S. Regulatory T cells: key controllers of immunologic self-tolerance. *Cell* 2000; **101**: 455–458.
39 Shevach EM. CD4+ CD25+ suppressor T cells: more questions than answers. *Nat Rev Immunol* 2002; **2**: 389–400.
40 Li W, Asokan A, Wu Z, Van Dyke T, DiPrimio N, Johnson JS *et al.* Engineering and selection of shuffled AAV genomes: a new strategy for producing targeted biological nanoparticles. *Mol Ther* 2008; **16**: 1252–1260.
41 Koga T, Koshiyama Y, Gotoh T, Yonemura N, Hirata A, Tanihara H *et al.* Coinduction of nitric oxide synthase and arginine metabolic enzymes in endotoxin-induced uveitis rats. *Exp Eye Res* 2002; **75**: 659–667.
42 Kügler S, Lingor P, Schöll U, Zolotukhin S, Bähr M. Differential transgene expression in brain cells *in vivo* and *in vitro* from AAV-2 vectors with small transcriptional control units. *Virology* 2003; **311**: 89–95.
43 Auricchio A, Hildinger M, O'Connor E, Gao GP, Wilson JM. Isolation of highly infectious and pure adeno-associated virus type 2 vectors with a single-step gravity-flow column. *Hum Gene Ther* 2001; **12**: 71–76.
44 Auricchio A, O'Connor E, Hildinger M, Wilson JM. A single-step affinity column for purification of serotype-5 based adeno-associated viral vectors. *Mol Ther* 2001; **4**: 372–374.
45 Sugano E, Tomita H, Ishiguro S, Abe T, Tamai M. Establishment of effective methods for transducing genes into iris pigment epithelial cells by using adeno-associated virus type 2. *Invest Ophthalmol Vis Sci* 2005; **46**: 3341–3348.
46 Papathanasiou ES, Peachey NS, Goto Y, Neafsey EJ, Castro AJ, Kartje GL. Visual cortical plasticity following unilateral sensorimotor cortical lesions in the neonatal rat. *Exp Neurol* 2006; **199**: 122–129.
47 Iwamura Y, Fujii Y, Kamei C. The effects of certain H(1)-antagonists on visual evoked potential in rats. *Brain Res Bull* 2003; **61**: 393–398.
48 Boettler T, Spangenberg HC, Neumann-Haefelin C, Panther E, Urbani S, Ferrari C *et al.* T cells with a CD4+CD25+ regulatory phenotype suppress *in vitro* proliferation of virus-specific CD8+ T cells during chronic hepatitis C virus infection. *J Virol* 2005; **79**: 7860–7867.

Experimental Eye Research 90 (2010) 429–436

Contents lists available at ScienceDirect

Experimental Eye Research

journal homepage: www.elsevier.com/locate/yexer

Channelrhodopsin-2 gene transduced into retinal ganglion cells restores functional vision in genetically blind rats☆

Hiroshi Tomita [a,*], Eriko Sugano [a], Hitomi Isago [a,b], Teru Hiroi [a], Zhuo Wang [a], Emi Ohta [a], Makoto Tamai [b]

[a] *Tohoku University, Institute for International Advanced Interdisciplinary Research, 4-1 Seiryo-machi, Aoba-ku, Sendai, 980-8575 Japan*
[b] *Tohoku University Graduate School of Medicine, Japan*

ARTICLE INFO

Article history:
Received 17 July 2009
Accepted in revised form 10 December 2009
Available online 27 December 2009

Keywords:
channelrhodopsin-2
Royal College of Surgeons rat
retinal ganglion cells
photoreceptor degeneration
visually evoked potential
retinitis pigmentosa
adeno-associated virus vector

ABSTRACT

To test the hypothesis that transduction of the channelrhodopsin-2 (*ChR2*) gene, a microbial-type rhodopsin gene, into retinal ganglion cells of genetically blind rats will restore functional vision, we recorded visually evoked potentials and tested the experimental rats for the presence of optomotor responses. The N-terminal fragment of the *ChR2* gene was fused to the fluorescent protein Venus and inserted into an adeno-associated virus to make AAV2-ChR2V. AAV2-ChR2V was injected intravitreally into the eyes of 6-month-old dystrophic RCS (rdy/rdy) rats. Visual function was evaluated six weeks after the injection by recording visually evoked potentials (VEPs) and testing optomotor responses. The expression of *ChR2V* in the retina was investigated histologically. We found that VEPs could not be recorded from 6-month-old dystrophic RCS rats that had not been injected with AAV2-ChR2V. In contrast, VEPs were elicited from RCS rats six weeks after injection with AAV2-ChR2V. The VEPs were recorded at stimulation rates <20 Hz, which was the same as that of normal rats. Optomotor responses were also significantly better after the AAV2-ChR2V injection. Expression of ChR2V was observed mainly in the retinal ganglion cells. These findings demonstrate that visual function can be restored in blind rats by transducing the *ChR2V* gene into retinal ganglion cells.

1. Introduction

Channelrhodopsin-2 (ChR2), cloned from the green algae *Chlamydomonas reinhardtii*, is classified as a microbial-type rhodopsin that can be activated by specific wavelengths of light (Nagel et al., 2003; Sineshchekov et al., 2002; Suzuki et al., 2003). ChR2 is similar to bacteriorhodopsin (Oesterhelt and Stoeckenius, 1973), which uses an attached chromophore to absorb photons. A reversible photoisomerization of the all-trans isoform of retinaldehyde changes its conformation, and this directly induces ion movement through the membrane (Oesterhelt, 1998). It is this specific feature that allows ChR2 to function as a cation channel after exposure to light (Nagel et al., 2003).

Retinitis pigmentosa (RP) is a retinal degenerative disease that is associated with a progressive loss of photoreceptor cells resulting in a loss of peripheral visual fields, then central vision, and finally blindness. Mutations of a number of genes have been shown to cause RP, and these genes are mainly related to the phototransduction pathway (RetNet; http://www.sph.uth.tmc.edu/Retnet/). Unfortunately, these findings have not led to a successful way to treat or prevent RP. A new strategy for restoring vision has been recently investigated, viz., transduction of the *channelrhodopsin-2* (*ChR2*) gene into genetically blind mice (Bi et al., 2006). These experiments have been performed on animals that have the same mutation as humans with retinitis pigmentosa (Bowes et al., 1990; Pittler and Baehr, 1991). We have also reported that the intravitreal injection of the *ChR2* gene into older dystrophic Royal College of Surgeons (RCS) rats (Mullen and LaVail, 1976), an animal model of recessively inherited retinitis pigmentosa (D'Cruz et al., 2000; Gal et al., 2000), restored functional vision (Tomita et al., 2007). These observations suggested that transduction of the *ChR2* gene would provide a new method for treating eyes with RP that is independent of the etiology of the retinal degeneration.

Flannery and Greenberg (2006) reported that behavioral testing would be necessary to determine if the use of *ChR2* was a viable

☆ Grant Information: This work was supported in part by Grants-in-Aid for Scientific Research from the Ministry of Education Science and Culture (No. 20791241, 21791664, 21200022), Ministry of Health, Labor and Welfare, Comprehensive Support Programs for Creation of Regional Innovation Science and Technology Incubation Program of the Japanese Government, Japanese Retinitis Pigmentosa Society, and Sumitomo Foundation.

* Corresponding author. Tel./fax: +81 22 717 8207.
E-mail address: hiroshi-tomita@iiare.tohoku.ac.jp (H. Tomita).

0014-4835/$ – see front matter © 2009 Elsevier Ltd. All rights reserved.
doi:10.1016/j.exer.2009.12.006

strategy for restoring functional vision to blind animals. Lagali et al. (2008) reported that ON-bipolar cells that were engineered to be photosensitive by the transfer of the ChR2 gene restored behavioral responses to genetically blind mice. When the *ChR2* gene was transduced into ON-bipolar cells, the retinal ON pathway was selectively activated by light. This is a reasonable way of activating the normal retinal ON pathway, although some methodological difficulties are still present when clinical applications are considered, e.g., the mechanism of gene transfer into ON-bipolar cells. Retinal ganglion cells are good candidates for receiving the ChR2 gene because target genes can be easily transduced into them. We have shown that a single injection of an AAV vector including ChR2 made it possible to change about 30% of all retinal ganglion cells to photosensitive ganglion cells. Recently it was reported that the ectopic expression of melanopsin in the retinal ganglion cells of retinal degeneration mice results in functional vision (Lin et al., 2008). In the same way, it is important to determine whether the ChR2 gene can restore functional vision when transferred retinal ganglion cells.

Thus, the purpose of this study was to determine whether transduction of the *ChR2* gene into retinal ganglion cells of blind RCS rats can restore functional vision. We used visually evoked responses and optomotor responses to assess the functional condition of the visual system. We found that AAV2-mediated *ChR2* transfer can lead to recovery of not only electrophysiological but also optokinetic responses.

2. Materials and methods

The procedures used on the animals in these experiments were in accordance with the ARVO Statement for the Use of Animals in Ophthalmic and Vision Research and the Guidelines for Animal Experiments of Tohoku University.

2.1. Experimental animals

The experiments were conducted on 6-month-old male RCS rats; 18 dystrophic (rdy/rdy), and 4 non-dystrophic (+/+). The rats were obtained from CLEA Japan, Inc. (Tokyo, Japan).

2.2. Vector construction

The construction of the vector expressing ChR2 and the preparation of the vector for injection have been described in detail (Sugano et al., 2005; Tomita et al., 2007). In brief, the N-terminal fragment (residues 1-315; GenBank Accession No. AF461397) of the *ChR2* gene was fused to a fluorescent protein, Venus, in frame at the end of the *ChR2* coding fragment. Then ChR2-Venus (ChR2V) was introduced into the EcoRI and Hind III sites of the 6P1 plasmid (Kugler et al., 2003). The synapsin promoter was exchanged for a hybrid CMV enhancer/chicken β-actin promoter (CAG) (Niwa et al., 1991). The AAV2-ChR2V vector was purified by a single-step column purification method of Auricchio et al. (Auricchio et al., 2001; Sugano et al., 2005).

2.3. AAV vector injection

The method used to inject the AAV-ChR2V vector into the vitreous of both eyes of 6-month-old RCS (rdy/rdy) rats has been described in detail (Tomita et al., 1999, 2007). In brief, rats were anesthetized by an intramuscular injection of a mixture of ketamine (66 mg/ml) and xylazine (33 mg/kg). Under an operating microscope, a small incision was made in the conjunctiva to expose the sclera, and 5 μl of a viral vector suspension at a concentration of $1–10 \times 10^{12}$ genomic particles/ml was injected into the center of the vitreous cavity through the ora serrata with a 32 gauge needle on a 10 μl Hamilton syringe (Hamilton Company, Reno, NV).

2.4. Recording visually evoked potentials (VEPs)

VEPs were recorded before and at one week after the injection of AAV-ChR2V vector with a Neuropack system (MEB-9102; Nihon Kohden, Tokyo, Japan) as described in detail (Tomita et al., 2007). The method of recording was derived from a combination of the protocols used by Papathanasiou et al. (2006) and Iwamura et al. (2003). Briefly, at least seven days before the recordings, silver–silver chloride electrodes were implanted epidurally 7 mm behind the bregma and 3 mm lateral to the midline of both hemispheres. A reference electrode was implanted epidurally on the midline 12 mm posterior to the bregma.

Under ketamine–xylazine anesthesia, the eye was stimulated with 20 ms duration 0.5 Hz photic stimuli. The photic stimuli were generated by pulse activation of a blue light-emitting diode (LED) with light-emitting wavelengths of 435–500 nm (peak at 470 nm). A white LED was used to determine the spectral responsiveness (white LEDs include all wavelengths). The high and low band-pass filters of the amplifier were set to 50 kHz and 0.05 kHz, respectively. One hundred consecutive responses were averaged for each VEP. We also investigated the changes of the VEP responses elicited by a train of stimulus frequencies of 1–50 Hz with a pulse duration of 10 ms.

The stimulus light intensity was measured by a laser power meter (Lasercheck, Edomond Optics, Japan).

2.5. Spectral responsivity of eye after transduction of ChR2V

To investigate the spectral responsivity of the retinas transduced with *ChR2V*, VEPs were elicited by different wavelength stimuli of 1 mW/cm^2. The wavelengths were isolated by band-pass filters (FUJIFILM Japan, Tokyo, Japan; Fig. 1A).

2.6. Behavioral assessments

The behavioral assessments were performed in a head-tracking instrument (Hayashi Seisakusyo, Kyoto, Japan). The instrument consisted of a circular drum rotating around the animal (Cowey and Franzini, 1979; Haruta et al., 2004; Lund et al., 2001). We covered the circular rotating drum with a transparent blue filter (Ultra color filter #67, Toshiba, Japan; filter transmits wavelengths <560 nm) because of the spectral absorption of ChR2. The vertical blue and black stripes subtended an angle of 10°, and the rotation speed was changed from 0 to 0.5, 2, 4, and 8 rpm. The spatial frequency corresponds to 0.05 cycle/degree, but the stimulus spatial frequency will change slightly with rat head position because the animal can freely move on the platform. The luminosity at the center of the holding chamber was set to 500 (1 mW/cm^2), 300 (0.55 mW/cm^2), and 100 lux (0.19 mW/cm^2). Dystrophic and control RCS rats were tested for 4 min at each speed before and after the ChR2 gene transfer.

The head movements of the animals were recorded by a video camera mounted above the apparatus. All movements were recorded at a rate of 29.95 frames/s. The number of movements was analyzed with movement-sensitive software (Move-tr/2D ver.7.0, Library, Tokyo). We made three marks; on the nose, the neck, and the waist of the rat on the software. The marked points were selected in the area that had a distinct color contrast to make it easy to trace them automatically. The software produced the angle of the three marked points. All of the angular movements >5° were considered to be tracking movements if the direction corresponded with the movement of the rotating stimulus. Large movements

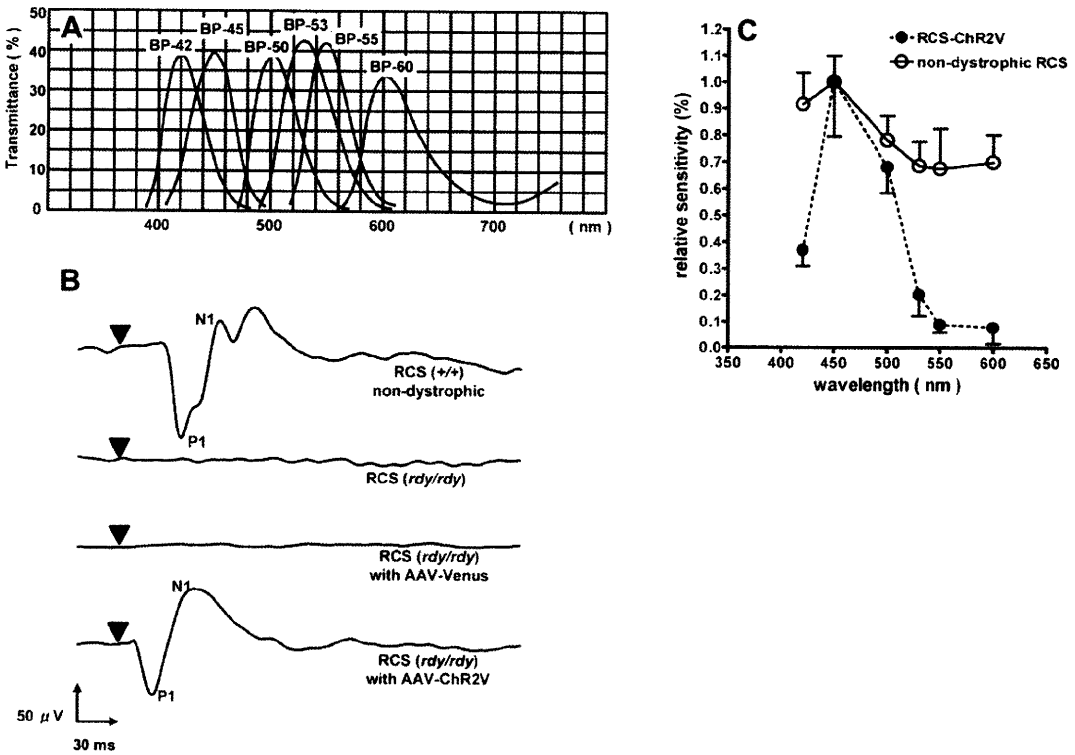

Fig. 1. Spectral responsivity of RCS rats transduced with the *ChR2V* gene. Different parts of the spectrum were isolated by six band-pass filters. A. Band passes for the six band-pass filters used to isolate different wavelengths of the visible spectrum. B. Typical waveforms of the VEPs elicited by 3500 lux stimuli emitted by blue LEDs (435–500 nm, peak at 470 nm). Upper: VEPs from a non-dystrophic rat; VEPs from a dystrophic rat without *ChR2V*; VEPs from a dystrophic rat with *Venus*. Lower: from a dystrophic rat with the *ChR2V* gene. C. Spectral responsiveness of eyes after transduction of *ChR2V* and of eyes of non-dystrophic rats. Amplitudes of VEPs elicited at the different wavelengths at the intensity of 1 mW/cm^2. The relative responses to the amplitude of the stimuli with a 450 nm band-pass filter were plotted. VEPs were recorded by stimuli delivered through each band-pass filter (open circles): non-dystrophic RCS rats ($n = 4$), (closed circles): dystrophic RCS rats with ChR2V ($n = 8$). Error bars represent standard deviations.

with movements of the body of the animal were not counted. The number of movements at 0 rpm was subtracted from that at each rotation speed.

2.7. Retrograde labeling of retinal ganglion cells (RGCs) with fluorogold

To identify the RGCs in the ganglion cell layer (GCL), the RGCs were retrogradely labeled seven days before the rats were sacrificed. The labeling was done by injecting 4 μl of 2% aqueous fluorogold (FG; Fluorochrome, Englewood, CO; Brecha and Weigmann, 1994) containing 1% dimethylsulfoxide into the superior colliculus with a 32 G needle on a Hamilton syringe.

2.8. ChR2V expression in retina

Sixteen weeks after the injection of AAV-ChR2V, rats ($n = 4$) were sacrificed and the eyes were removed and fixed in 4% paraformaldehyde in 0.1 M phosphate buffer. The ipsilateral retinas were isolated and flat-mounted on microscope slides. The fluorogold-labeled and ChR2-expressing cells were counted in 12 distinct areas of the retina (three areas in each quadrant starting 1 mm from the optic nerve) to evaluate the transduction efficiency. Two of the contralateral eyes were embedded in OCT compound (Sakura, Tokyo, Japan) after immersion in 30% sucrose solution in PBS. Fifteen micrometer retinal sections were cut and mounted on slides. The slides of retinal whole mounts and sections were covered with Vectashield medium (Vector Laboratories, Burlingame, CA). The Venus fluorescence was examined with a fluorescence microscope, Axiovert40 (Carl Zeiss).

2.9. Histological studies of the retina

Another two of the eyes were used for paraffin-embedded sections to examine histological changes induced by the expression of ChR2. Analyses of the retinal morphologies in ChR2V−/− and ChR2V+/− rats were performed as described Li et al. (2007). In brief, rats were sacrificed by asphyxiation with carbon dioxide after the induction of photoreceptor degeneration. The eyes were enucleated, fixed, and embedded in paraffin. Three-micrometer thick sections of retinas were cut along the vertical meridian and stained with hematoxylin and eosin to allow examination of the retina in the superior and inferior hemispheres (LaVail et al., 1992).

2.10. Statistical analyses

Statistical analyses was performed using GraphPad Prism software (GraphPad Software, San Diego, CA). The criterion for statistical significance was $P < 0.05$.

3. Results

3.1. Spectral responsivity of ChR2V-expressing retinas

To investigate the spectral responsivity of ChR2V-expressing retinas, visually evoked potentials were elicited by light filtered

through six band-pass filters that isolated different parts of the spectrum (Fig. 1A). Typical waveforms elicited by light filtered through the BP-450 nm filter in rats with or without ChR2V are shown in Fig. 1B. Large amplitude VEPs were recorded from 6-month-old non-dystrophic RCS rats, but no response was elicited from untreated 6-month-old dystrophic RCS rats (Fig. 1B). However, six weeks after the injection of AAV-ChR2V, large (123.0 ± 13.5 μV) VEPs were recorded when the eye was stimulated with a stimulus intensity of 3500 lux (Fig. 1B). The largest amplitude was elicited by the wavelength of 450 nm (Fig. 1C), and VEPs were evoked by stimuli whose wavelengths were ≤550 nm.

3.2. Changes in VEP amplitude at different times after injection of AAV2-ChR2V

VEPs in RCS rats injected with AAV2-ChR2V were first detected two weeks after the injection (Fig. 2A). Thereafter, the amplitude progressively increased up to five weeks post-injection when the mean amplitude was 118.4 μV (Fig. 2A). In dystrophic RCS rats of the same age, VEPs were not detected with the same stimuli (noise level 5 μV). With increasing stimulus intensities, the amplitudes of the VEPs increased and the latencies of P1 decreased (Fig. 2B). Interestingly, the latencies of P1 in the *ChR2*-transduced RCS rats (24.68 ± 2.78 ms) were shorter than those in non-dystrophic RCS rats (49.43 ± 1.21 ms; $P < 0.0001$; un-paired t test; Fig. 2C).

3.3. Changes of VEPs responses by different frequencies of light stimulation

VEPs elicited by different frequencies of light stimulation were recorded from wild-type and dystrophic rats transduced with the *ChR2V* gene. VEPs were recorded from both types of rats when the stimulus frequencies were <20 Hz (Fig. 3A). Responses could not be detected in either type of rat when the stimulus frequencies were 40 Hz and 50 Hz. The responses from both rats were well fit by the Boltzmann fitting curve (Fig. 3B). The amplitudes of the VEPs in rats with *ChR2V* were not affected by a 200 ms interval of a train of light stimuli (Fig. 3C). These results indicated that the responsivity to light allowed by the transduction of *ChR2V* is similar to that in wild-type rats.

3.4. Behavioral assessment by optomotor responses

To determine whether transduction of the *ChR2* gene restored functional vision, optomotor responses were recorded from non-dystrophic normal (Fig. 4A), dystrophic (Fig. 4B) and *ChR2*-transduced RCS rats (Fig. 4C). Preliminary experiments showed that when the angle of the neck moved over 5°, the movements were well correlated with the rotation speed in the non-dystrophic RCS (+/+) rats (Fig. 4D). Therefore, we counted the number of neck movements over 5°. The score in 30-week-old uninjected dystrophic rats at 2 rpm was 3.00 ± 3.64, while that in 30-week-old rats six weeks post-injection was significantly higher 13.31 ± 5.82 ($P < 0.0006$; Fig. 4E). Although non-dystrophic rats (+/+) responded to the rotation even at speeds of 2 rpm at 300 lux and to 4 rpm at 100 lux (Fig. 4F), the rats with the transduced *ChR2V* gene did not respond to the lower light intensities (Fig. 4G).

3.5. ChR2V expression in retina

Histological examination of flat mounts of the retina showed cells over a wide area of the retina had been retrogradely labeled

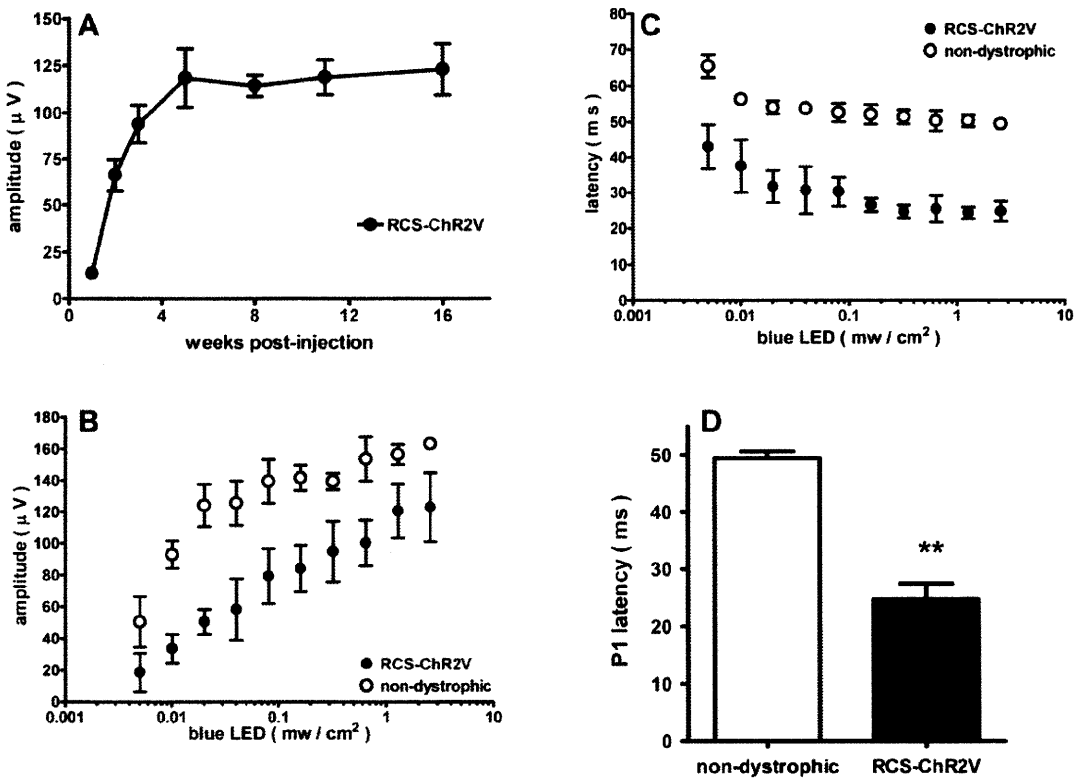

Fig. 2. VEPs recorded from RCS rats transduced with the *ChR2V* gene. A. Changes in amplitude at different weeks after the injection of AAV-ChR2V. B. Changes in amplitude (P1–N1) and latency (P1) elicited by different stimulus intensities. Blue LEDs (435–500 nm, Peak at 470 nm) were used to elicit the VEPs. C. Differences of the P1 latency between non-dystrophic and ChR2V-transduced dystrophic rats. Error bars represent the standard deviation of the mean. The statistical evaluation was performed using the un-paired t test (dystrophic RCS with ChR2V; $n = 8$, non-dystrophic RCS; $n = 4$, $^{**}P < 0.0001$).

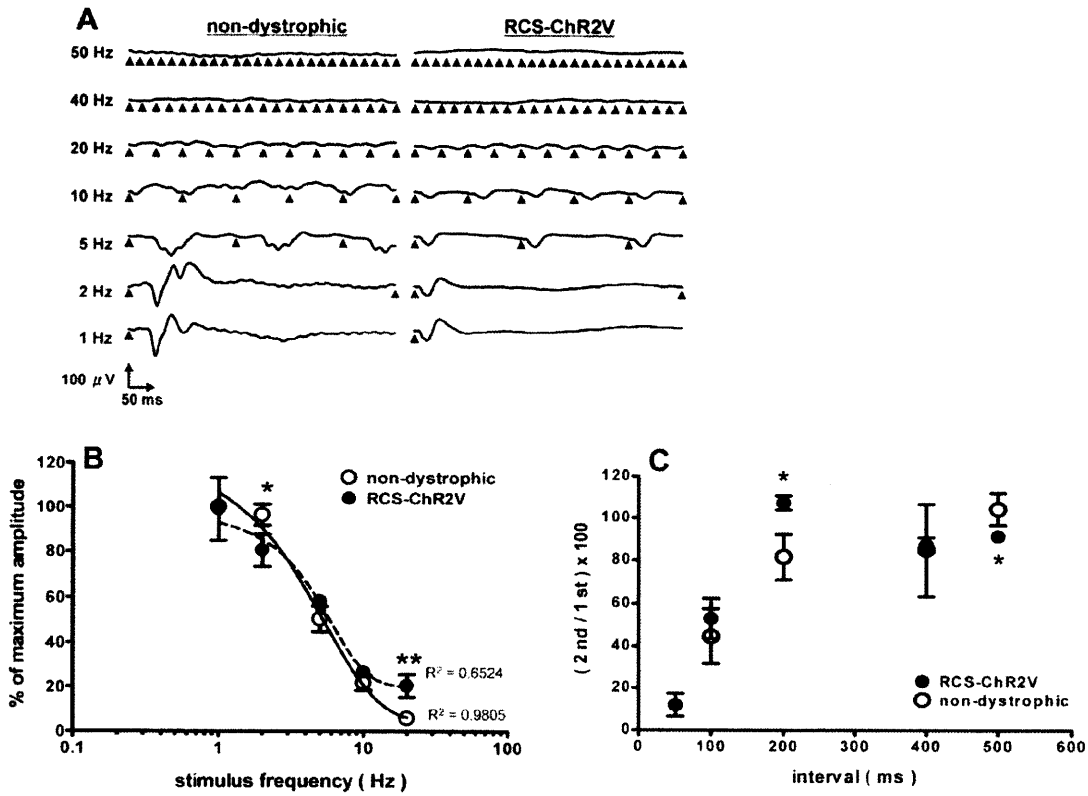

Fig. 3. Changes of responsivity in VEPs elicited by different stimulus frequencies. A. Typical VEP waveforms elicited by different stimulus frequencies. B. Changes in VEP amplitude elicited by different stimulus frequencies. Data are expressed as percentages of the amplitude at 1 Hz. The amplitude recruitment curve was fitted to the Boltzmann model. C. Changes in VEP amplitude elicited by different stimulus trains. Data are expressed as a percentage of the amplitude elicited by the first stimulus. Photic stimuli were generated by a blue LED (435–500 nm, peak at 470 nm) at 3500 lux. The statistical evaluation was performed using the un-paired *t* test (dystrophic RCS with ChR2V; $n = 8$, non-dystrophic RCS; $n = 4$, $^{*}P < 0.05$, $^{**}P < 0.01$).

with Fluorogold (Fig. 5A). These cells were considered to be RGCs (Fig. 5B). Merged images showed that the expression of *ChR2V* was mainly in the RGCs (Fig. 5C). When the AAV-Venus vector was injected, Venus fluorescence was also observed in the RGCs, but the Venus protein was localized in the cell body, which was completely different from those injected with AAV-ChR2V (Fig. 5D). Cryosections showed that the labeled cells were observed in the ganglion cell layer (Fig. 5E and F) and some of them were in the inner nuclear layer (Fig. 5F). Photoreceptor cells were not seen in the retinas of the RCS rats (Fig. 5G). The number of fluorogold-labeled cells, which are most likely retinal ganglion cells, was 2531.8 ± 214.8. The number of double-labeled cells was 710.6 ± 117.7. Thus, the transduction efficiency was about 28.3% (Fig. 5H). Paraffin sections also showed no difference in the thickness of the photoreceptor layer between non-injected and AAV-ChR2-injected retinas (Fig. 5I and J).

4. Discussion

Our results demonstrated that VEPs can be recorded from genetically blind RCS rats that expressed the *ChR2* gene, and the maximum response was elicited by stimuli with a peak wavelength at 450 nm. This agrees with an earlier report that the peak spectral absorption of *ChR2* is approximately at 460 nm (Nagel et al., 2003). In addition, VEPs were elicited by stimuli up to 550 nm, whereas non-dystrophic RCS rats responded to wavelengths over 600 nm. This ability of normal rats to respond to longer wavelengths is probably because they have two cone photopigments with peak absorbances at 359 nm (Deegan and Jacobs, 1993; Yokoyama et al., 1998) and at 510 nm (Neitz and Jacobs, 1986). Therefore, the spectral responsivity spectrum of rats transduced with the *ChR2* gene is somewhat narrower than that of non-dystrophic rats, and this is due to the presence of only channelrhodopsin-2 in the retina.

Distinct VEPs were first recorded at two weeks post-injection. The amplitudes of the VEPs of dystrophic RCS rats carrying the *ChR2* gene in their RGCs gradually increased up to six weeks post-injection. Interestingly, the implicit times (ITs) of the VEPs were shorter than those of non-dystrophic rats. The cause of the shorter ITs was most likely because the neural signals were transduced in the RGCs, and the signals did not have to pass through the inner retinal network. These results suggest that the retinal ganglion cells became photosensitive by the expression of the *ChR2* gene, and the signals generated in the ganglion cells were transmitted to the visual cortex from the RGCs.

We compared the responsivity to different frequencies of light stimulation between non-dystrophic RCS rats and ChR2V-injected rats. The RCS rat with the *ChR2* gene responded up to 20 Hz, which was same as that from non-dystrophic RCS rat. Jehle et al. (2008) reported that steady-state VEPs could elicited by a stimulus frequency of 38 Hz and distinct amplitudes were observed at 19 Hz. The responsivity was slightly higher than our results (20 Hz). The maximum amplitude evoked from RCS rats with *ChR2* was about 50% of that from non-dystrophic RCS rats at 1 Hz. The lower amplitude from rats with ChR2V was probably due to the gene transduction efficiency in the retinal ganglion, which was about 30% of the retinal ganglion cells in this study. We previously

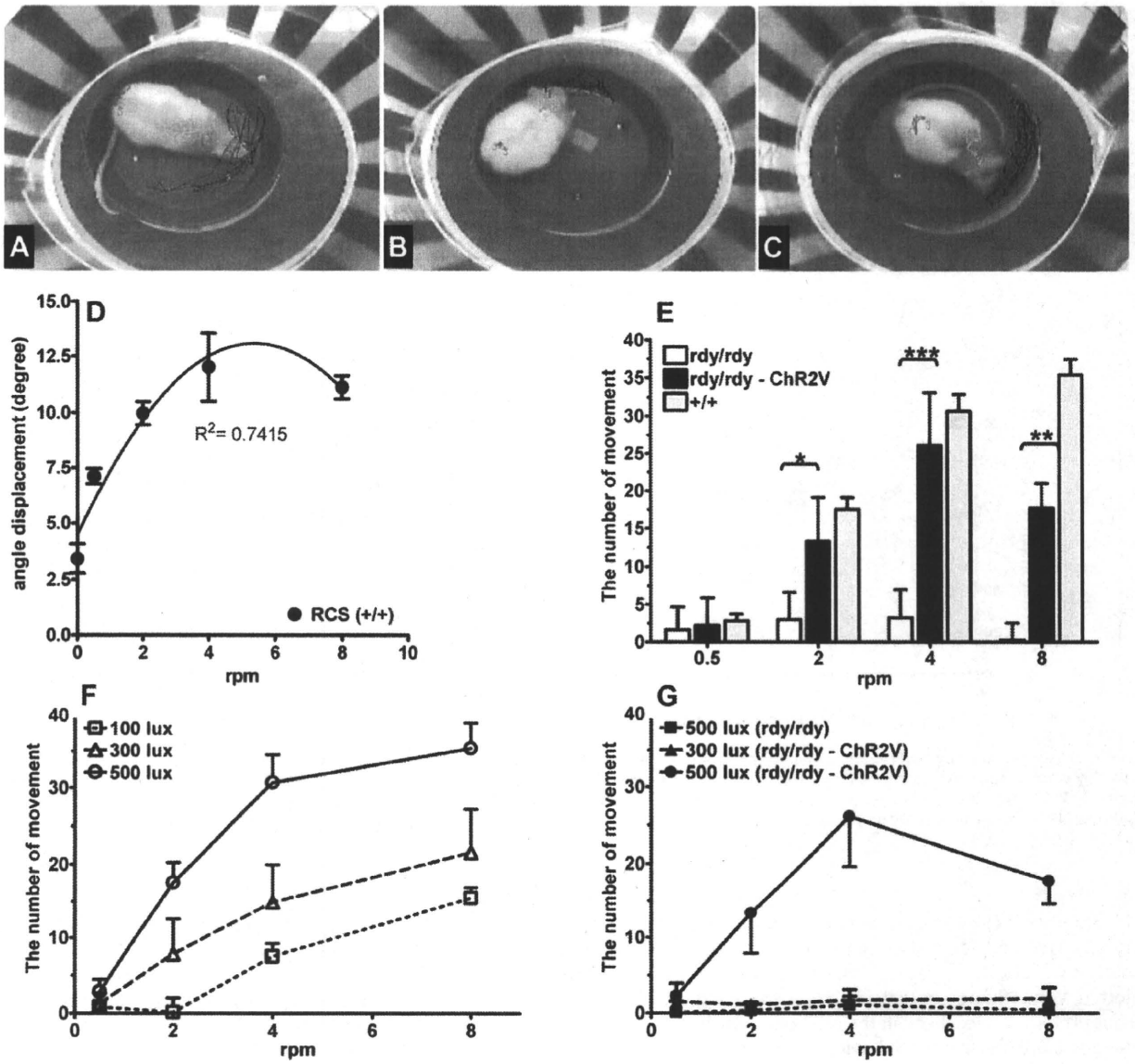

Fig. 4. Behavioral assessment of dystrophic RCS rats and *ChR2V*-transduced rats. The traces of each marked point in non-dystrophic (A), dystrophic (B) and ChR2V-transduced dystrophic (C) rats during a test at 4 rpm. The red, green and blue lines correspond to the marks on the nose, the neck and the waist, respectively. Each score was calculated by subtracting the number of movements at 0 rpm. The angular displacement of each movement in the non-dystrophic rats (D). The luminosity at the center of the holding chamber was set to 500 lux (E). Effects of light intensity on the movements of non-dystrophic (F) and dystrophic RCS rats with ChR2V (G). The score of the non-dystrophic rats increased with increasing light intensities. The drum with black and transparent blue stripes was rotated at speeds of 0, 0.5, 2, 4 and 8 rpm. Error bars represent standard deviations of the means (un-paired *t* test; $n = 8$, $^{*}P < 0.05$, $^{**}P < 0.01$, $^{***}P < 0.001$).

reported that the transduction efficiency of 10-month-old RCS rats was about 30% (Tomita et al., 2007). The transduction efficiency in the 6-month old rats we used in this study was approximately the same. The AAV we used in this study required host-cell synthesis of the complementary strand for transduction. The failure to undergo viral second-strand synthesis leads to a lower efficiency of transgene expression (Ferrari et al., 1996; Fisher et al., 1996). The use of self-complementary AAV (scAAV) vectors that do not require synthesis of the complementary strand for transgene expression can circumvent this problem. Thus, this method has the possibility of being more efficient and acting more rapidly (Andino et al., 2007; Jayandharan et al., 2008; McCarty et al., 2001).

To determine the functional visual capabilities of *ChR2*-transduced RCS rats, we investigated their optomotor responses (Haruta et al., 2004; Lund et al., 2001). The a-wave of the ERG is an indicator of photoreceptor function, and it disappears by 80–100 days in dystrophic RCS rats (Bush et al., 1995; Sauve et al., 2004). However, the activity of single ganglion cells could be recorded from the optic tract of RCS rats even after the electroretinogram (ERG) could not be recorded (Cicerone et al., 1979). Assessments of their visual sensitivity as determined by electric potentials recorded from the superior colliculus indicated that the sensitivity progressively decreased to reach a plateau at 180–240 days (Sauve et al., 2001). Therefore, we chose 8-month-old RCS rats (2 months after the injection of AAV-ChR2V) for the behavioral assessments. The behavioral scores of the ChR2-transduced RCS rats were significantly higher than those of untreated rats. We also found that the scores of the ChR2-transduced RCS rats were affected by the light intensity in the drum (Fig. 4F).

Lagali et al. (2008) reported that ON-bipolar cells that were engineered to be photosensitive by the transduction of the ChR2

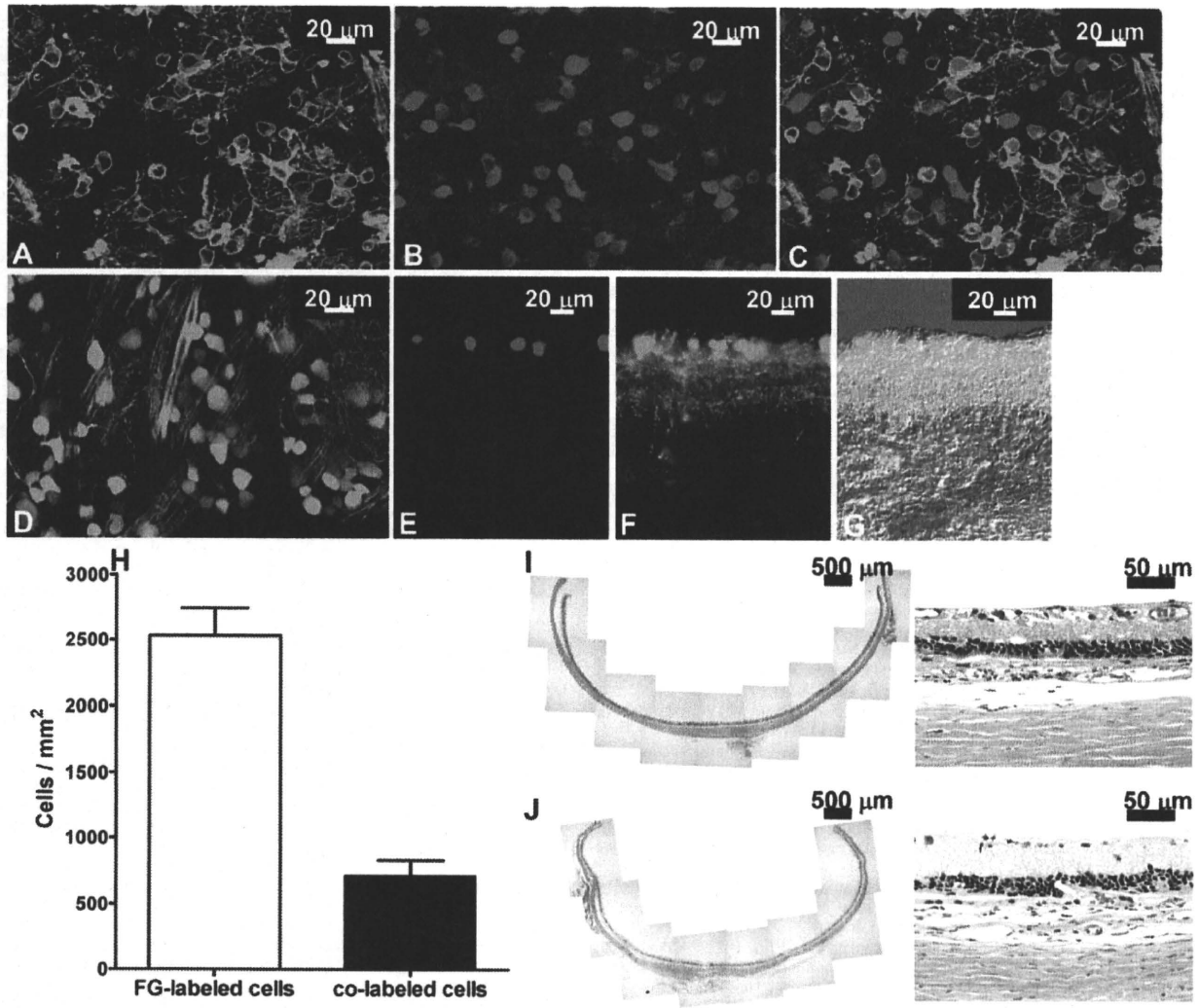

Fig. 5. Expression of ChR2V in the retina. Histological examination of retinas of rats injected with AAV-ChR2V at 16 weeks after the injection. A. Flat-mounted section showing the expression of *ChR2V* gene by green fluorescence. B. Retinal ganglion cells that were retrogradely labeled with fluorogold. C. Merged photograph showing both fluorogold and ChR2V. Many cells are double-labeled. D. Flat-mounted section from a rat transduced with AAV-Venus as a control vector. E. Merged photograph of the Nomarski image, Fluorogold (F) and ChR2V (G). H. The transduction efficiency of ChR2 gene into RGCs ($n = 8$). Hematoxilin–eosin sections from both non-injected RCS rats (I) and AAV-ChR2V-injected RCS rats (J) revealed a loss of photoreceptors in the entire retina.

gene restored visual function to eyes with retinal degeneration. ON and OFF bipolar cells receive synaptic input from photoreceptors. The ON-bipolar cells are one of the candidate cells for receipt of the ChR2 gene because ChR2 can elicit light-on responses. However, some reports have been published that retinal remodeling is triggered in bipolar cells and horizontal cells following photoreceptor degeneration (Marc et al., 2003, 2007; Strettoi and Pignatelli, 2000; Strettoi et al., 2002, 2003). Therefore, the function of the inner retinal layers, including the ON-bipolar pathway, might have some differences from that in normal eyes.

We found that behavioral responses could not be elicited by stimulus intensities <300 lux, although rats could respond at 500 lux. The 500 and 300 lux intensities correspond to about 2.25×10^{15} and 1.24×10^{15} photon/cm^2, respectively. The critical light intensity that elicited behavioral responses in rats with ChR2 transduced into their RGCs was expected to be 2.25×10^{15} photon/cm^2 s, which was close to the light level (3×10^{15} photon/cm^2 s) (Lagali et al., 2008) reported in the behavioral experiments performed on mice with ChR2 transduced into their ON-bipolar cells.

Our findings that ChR2 transduced-ganglion cells could restore visual function both electrophysiologically and behaviorally demonstrate that ganglion cells should also be considered as promising candidates cells for restoring vision via transfer of the ChR2 gene.

Acknowledgements

We thank Prof. Duco Hamasaki for discussions and editing the manuscript.

References

Andino, L.M., Conlon, T.J., Porvasnik, S.L., Boye, S.L., Hauswirth, W.W., Lewin, A.S., 2007. Rapid, widespread transduction of the murine myocardium using self-complementary Adeno-associated virus. Genet. Vaccines Ther. 5, 13.

Auricchio, A., Hildinger, M., O'Connor, E., Gao, G.P., Wilson, J.M., 2001. Isolation of highly infectious and pure adeno-associated virus type 2 vectors with a single-step gravity-flow column. Hum. Gene Ther. 12, 71–76.

Bi, A., Cui, J., Ma, Y.P., Olshevskaya, E., Pu, M., Dizhoor, A.M., Pan, Z.H., 2006. Ectopic expression of a microbial-type rhodopsin restores visual responses in mice with photoreceptor degeneration. Neuron 50, 23–33.
Bowes, C., Li, T., Danciger, M., Baxter, L.C., Applebury, M.L., Farber, D.B., 1990. Retinal degeneration in the rd mouse is caused by a defect in the beta subunit of rod cGMP-phosphodiesterase. Nature 347, 677–680.
Brecha, N.C., Weigmann, C., 1994. Expression of GAT-1, a high-affinity gamma-aminobutyric acid plasma membrane transporter in the rat retina. J. Comp. Neurol. 345, 602–611.
Bush, R.A., Hawks, K.W., Sieving, P.A., 1995. Preservation of inner retinal responses in the aged Royal College of Surgeons rat. Evidence against glutamate excitotoxicity in photoreceptor degeneration. Invest. Ophthalmol. Vis. Sci. 36, 2054–2062.
Cicerone, C.M., Green, D.G., Fisher, L.J., 1979. Cone inputs to ganglion cells in hereditary retinal degeneration. Science 203, 1113–1115.
Cowey, A., Franzini, C., 1979. The retinal origin of uncrossed optic nerve fibres in rats and their role in visual discrimination. Exp. Brain Res. 35, 443–455.
D'Cruz, P.M., Yasumura, D., Weir, J., Matthes, M.T., Abderrahim, H., LaVail, M.M., Vollrath, D., 2000. Mutation of the receptor tyrosine kinase gene Mertk in the retinal dystrophic RCS rat. Hum. Mol. Genet. 9, 645–651.
Deegan 2nd, J.F., Jacobs, G.H., 1993. On the identity of the cone types of the rat retina. Exp. Eye Res. 56, 375–377.
Ferrari, F.K., Samulski, T., Shenk, T., Samulski, R.J., 1996. Second-strand synthesis is a rate-limiting step for efficient transduction by recombinant adeno-associated virus vectors. J. Virol. 70, 3227–3234.
Fisher, K.J., Gao, G.P., Weitzman, M.D., DeMatteo, R., Burda, J.F., Wilson, J.M., 1996. Transduction with recombinant adeno-associated virus for gene therapy is limited by leading-strand synthesis. J. Virol. 70, 520–532.
Flannery, J.G., Greenberg, K.P., 2006. Looking within for vision. Neuron 50, 1–3.
Gal, A., Li, Y., Thompson, D.A., Weir, J., Orth, U., Jacobson, S.G., Apfelstedt-Sylla, E., Vollrath, D., 2000. Mutations in MERTK, the human orthologue of the RCS rat retinal dystrophy gene, cause retinitis pigmentosa. Nat. Genet. 26, 270–271.
Haruta, M., Sasai, Y., Kawasaki, H., Amemiya, K., Ooto, S., Kitada, M., Suemori, H., Nakatsuji, N., Ide, C., Honda, Y., Takahashi, M., 2004. In vitro and in vivo characterization of pigment epithelial cells differentiated from primate embryonic stem cells. Invest. Ophthalmol. Vis. Sci. 45, 1020–1025.
Iwamura, Y., Fujii, Y., Kamei, C., 2003. The effects of certain H(1)-antagonists on visual evoked potential in rats. Brain Res. Bull. 61, 393–398.
Jayandharan, G.R., Zhong, L., Li, B., Kachniarz, B., Srivastava, A., 2008. Strategies for improving the transduction efficiency of single-stranded adeno-associated virus vectors in vitro and in vivo. Gene Ther. 15, 1287–1293.
Jehle, T., Wingert, K., Dimitriu, C., Meschede, W., Lasseck, J., Bach, M., Lagreze, W.A., 2008. Quantification of ischemic damage in the rat retina: a comparative study using evoked potentials, electroretinography, and histology. Invest. Ophthalmol. Vis. Sci. 49, 1056–1064.
Kugler, S., Lingor, P., Scholl, U., Zolotukhin, S., Bahr, M., 2003. Differential transgene expression in brain cells in vivo and in vitro from AAV-2 vectors with small transcriptional control units. Virology 311, 89–95.
Lagali, P.S., Balya, D., Awatramani, G.B., Munch, T.A., Kim, D.S., Busskamp, V., Cepko, C.L., Roska, B., 2008. Light-activated channels targeted to ON bipolar cells restore visual function in retinal degeneration. Nat. Neurosci. 11, 667–675.
LaVail, M.M., Unoki, K., Yasumura, D., Matthes, M.T., Yancopoulos, G.D., Steinberg, R. H., 1992. Multiple growth factors, cytokines, and neurotrophins rescue photoreceptors from the damaging effects of constant light. Proc. Natl. Acad. Sci. U.S. A. 89, 11249–11253.
Li, G., Anderson, R.E., Tomita, H., Adler, R., Liu, X., Zack, D.J., Rajala, R.V., 2007. Nonredundant role of Akt2 for neuroprotection of rod photoreceptor cells from light-induced cell death. J. Neurosci. 27, 203–211.
Lin, B., Koizumi, A., Tanaka, N., Panda, S., Masland, R.H., 2008. Restoration of visual function in retinal degeneration mice by ectopic expression of melanopsin. Proc. Natl. Acad. Sci. U.S.A. 105, 16009–16014.
Lund, R.D., Adamson, P., Sauve, Y., Keegan, D.J., Girman, S.V., Wang, S., Winton, H., Kanuga, N., Kwan, A.S., Beauchene, L., Zerbib, A., Hetherington, L., Couraud, P.O., Coffey, P., Greenwood, J., 2001. Subretinal transplantation of genetically modified human cell lines attenuates loss of visual function in dystrophic rats. Proc. Natl. Acad. Sci. U.S.A. 98, 9942–9947.
Marc, R.E., Jones, B.W., Watt, C.B., Strettoi, E., 2003. Neural remodeling in retinal degeneration. Prog. Retin. Eye Res. 22, 607–655.
Marc, R.E., Jones, B.W., Anderson, J.R., Kinard, K., Marshak, D.W., Wilson, J.H., Wensel, T., Lucas, R.J., 2007. Neural reprogramming in retinal degeneration. Invest. Ophthalmol. Vis. Sci. 48, 3364–3371.
McCarty, D.M., Monahan, P.E., Samulski, R.J., 2001. Self-complementary recombinant adeno-associated virus (scAAV) vectors promote efficient transduction independently of DNA synthesis. Gene Ther. 8, 1248–1254.
Mullen, R.J., LaVail, M.M., 1976. Inherited retinal dystrophy: primary defect in pigment epithelium determined with experimental rat chimeras. Science 192, 799–801.
Nagel, G., Szellas, T., Huhn, W., Kateriya, S., Adeishvili, N., Berthold, P., Ollig, D., Hegemann, P., Bamberg, E., 2003. Channelrhodopsin-2, a directly light-gated cation-selective membrane channel. Proc. Natl. Acad. Sci. U.S.A. 100, 13940–13945.
Neitz, J., Jacobs, G.H., 1986. Reexamination of spectral mechanisms in the rat (*Rattus norvegicus*). J. Comp. Psychol. 100, 21–29.
Niwa, H., Yamamura, K., Miyazaki, J., 1991. Efficient selection for high-expression transfectants with a novel eukaryotic vector. Gene 108, 193–199.
Oesterhelt, D., Stoeckenius, W., 1973. Functions of a new photoreceptor membrane. Proc. Natl. Acad. Sci. U.S.A. 70, 2853–2857.
Oesterhelt, D., 1998. The structure and mechanism of the family of retinal proteins from halophilic archaea. Curr. Opin. Struct. Biol. 8, 489–500.
Papathanasiou, E.S., Peachey, N.S., Goto, Y., Neafsey, E.J., Castro, A.J., Kartje, G.L., 2006. Visual cortical plasticity following unilateral sensorimotor cortical lesions in the neonatal rat. Exp. Neurol. 199, 122–129.
Pittler, S.J., Baehr, W., 1991. Identification of a nonsense mutation in the rod photoreceptor cGMP phosphodiesterase beta-subunit gene of the rd mouse. Proc. Natl. Acad. Sci. U.S.A. 88, 8322–8326.
Sauve, Y., Girman, S.V., Wang, S., Lawrence, J.M., Lund, R.D., 2001. Progressive visual sensitivity loss in the Royal College of Surgeons rat: perimetric study in the superior colliculus. Neuroscience 103, 51–63.
Sauve, Y., Lu, B., Lund, R.D., 2004. The relationship between full field electroretinogram and perimetry-like visual thresholds in RCS rats during photoreceptor degeneration and rescue by cell transplants. Vis. Res. 44, 9–18.
Sineshchekov, O.A., Jung, K.H., Spudich, J.L., 2002. Two rhodopsins mediate phototaxis to low- and high-intensity light in *Chlamydomonas reinhardtii*. Proc. Natl. Acad. Sci. U.S.A. 99, 8689–8694.
Strettoi, E., Pignatelli, V., 2000. Modifications of retinal neurons in a mouse model of retinitis pigmentosa. Proc. Natl. Acad. Sci. U.S.A. 97, 11020–11025.
Strettoi, E., Porciatti, V., Falsini, B., Pignatelli, V., Rossi, C., 2002. Morphological and functional abnormalities in the inner retina of the rd/rd mouse. J. Neurosci. 22, 5492–5504.
Strettoi, E., Pignatelli, V., Rossi, C., Porciatti, V., Falsini, B., 2003. Remodeling of second-order neurons in the retina of rd/rd mutant mice. Vis. Res. 43, 867–877.
Sugano, E., Tomita, H., Ishiguro, S., Abe, T., Tamai, M., 2005. Establishment of effective methods for transducing genes into iris pigment epithelial cells by using adeno-associated virus type 2. Invest. Ophthalmol. Vis. Sci. 46, 3341–3348.
Suzuki, T., Yamasaki, K., Fujita, S., Oda, K., Iseki, M., Yoshida, K., Watanabe, M., Daiyasu, H., Toh, H., Asamizu, E., Tabata, S., Miura, K., Fukuzawa, H., Nakamura, S., Takahashi, T., 2003. Archaeal-type rhodopsins in *Chlamydomonas*: model structure and intracellular localization. Biochem. Biophys. Res. Commun. 301, 711–717.
Tomita, H., Ishiguro, S., Abe, T., Tamai, M., 1999. Administration of nerve growth factor, brain-derived neurotrophic factor and insulin-like growth factor-II protects phosphate-activated glutaminase in the ischemic and reperfused rat retinas. Tohoku J. Exp. Med. 187, 227–236.
Tomita, H., Sugano, E., Yawo, H., Ishizuka, T., Isago, H., Narikawa, S., Kugler, S., Tamai, M., 2007. Restoration of visual response in aged dystrophic RCS rats using AAV-mediated channelopsin-2 gene transfer. Invest. Ophthalmol. Vis. Sci. 48, 3821–3826.
Yokoyama, S., Radlwimmer, F.B., Kawamura, S., 1998. Regeneration of ultraviolet pigments of vertebrates. FEBS Lett. 423, 155–158.

OPEN ACCESS Freely available online PLoS one

Visual Properties of Transgenic Rats Harboring the Channelrhodopsin-2 Gene Regulated by the Thy-1.2 Promoter

Hiroshi Tomita[1]*, Eriko Sugano[1], Yugo Fukazawa[4,5], Hitomi Isago[1,2], Yuka Sugiyama[8,10], Teru Hiroi[1], Toru Ishizuka[3], Hajime Mushiake[9], Megumi Kato[7], Masumi Hirabayashi[5,7], Ryuichi Shigemoto[4,5,6], Hiromu Yawo[3,8], Makoto Tamai[2]

1 International Advanced Interdisciplinary Research, Tohoku University, Sendai, Japan, **2** Department of Medical Biochemistry, Tohoku University Graduate School of Medicine, Sendai, Japan, **3** Department of Developmental Biology and Neuroscience, Tohoku University Graduate School of Life Sciences, Sendai, Japan, **4** Division of Cerebral Structure, National Institute for Physiological Sciences, Okazaki, Japan, **5** Sokendai, Kanagawa, Japan, **6** Solution-Oriented Research for Science and Technology, Kawaguchi, Japan, **7** Section of Mammalian Transgenesis, Center for Genetic Analysis of Behavior, National Institute for Physiological Sciences, Okazaki, Japan, **8** Tohoku University Basic and Translational Research Center for Global Brain Science, Sendai, Japan, **9** Department of Physiology, Tohoku University Graduate School of Medicine, Sendai, Japan, **10** Department of Physiology and Pharmacology, Tohoku University Graduate School of Medicine, Sendai, Japan

Abstract

Channelrhodopsin-2 (ChR2), one of the archea-type rhodopsins from green algae, is a potentially useful optogenetic tool for restoring vision in patients with photoreceptor degeneration, such as retinitis pigmentosa. If the ChR2 gene is transferred to retinal ganglion cells (RGCs), which send visual information to the brain, the RGCs may be repurposed to act as photoreceptors. In this study, by using a transgenic rat expressing ChR2 specifically in the RGCs under the regulation of a Thy-1.2 promoter, we tested the possibility that direct photoactivation of RGCs could restore effective vision. Although the contrast sensitivities of the optomotor responses of transgenic rats were similar to those observed in the wild-type rats, they were enhanced for visual stimuli of low-spatial frequency after the degeneration of native photoreceptors. This result suggests that the visual signals derived from the ChR2-expressing RGCs were reinterpreted by the brain to form behavior-related vision.

Citation: Tomita H, Sugano E, Fukazawa Y, Isago H, Sugiyama Y, et al. (2009) Visual Properties of Transgenic Rats Harboring the Channelrhodopsin-2 Gene Regulated by the Thy-1.2 Promoter. PLoS ONE 4(11): e7679. doi:10.1371/journal.pone.0007679

Editor: Eric Warrant, Lund University, Sweden

Received July 16, 2009; **Accepted** October 8, 2009; **Published** November 5, 2009

Funding: This work was supported in part by Grants-in-Aid for Scientific Research from the Ministry of Education, Culture, Sports, Science and Technology (MEXT) of Japan (No. 17390465, 17791217, 17659541), Science and Culture and Special Coordination Funds for Promoting Science and Technology of the Japanese Government, Strategic Research Program for Brain Sciences (SRPBS), Japanese Retinitis Pigmentosa Society (JRPS), and Suzuken Memorial Foundation. The funders had no role in study design, data collection and analysis, decision to publish, or preparation of the manuscript.

Competing Interests: The authors have declared that no competing interests exist.

* E-mail: hiroshi-tomita@iiare.tohoku.ac.jp

Introduction

Retinitis pigmentosa (RP) is a genetically heterogeneous disease characterized by degeneration of the retinal photoreceptor cells. A number of genes responsible for RP have been identified, most of them related to the phototransduction pathways. Patients who have such mutations experience night blindness, loss of their peripheral visual field, and loss of central vision [1]. Although the photoreceptor cells are degenerated in the eyes of RP patients with vision loss, other retinal neurons, including retinal ganglion cells (RGCs), are still preserved [2,3,4].

Channelrhodopsin-2 (ChR2), a rhodopsin identified in the green algae Chlamydomonas reinhardtii, is unique in that it acts as a directly light-gated cation-selective ion channel [5]. Several studies have revealed that neurons became photosensitive when transfected with the ChR2 gene [6,7]. In addition, Bi et al. reported that the transfer of ChR2 restored visually evoked cortical responses in blind mice [8]. We also observed restoration of visual response in genetically blind rats [9]. Following on the study of Bi et al. and our own research, we believe that, in addition to their native function of transmitting visual signals to the brain, RGCs are endowed with a photoreceptor-like function by the ChR2 gene. There are three types of RGCs in the mammalian retina: ON, OFF, and ON-OFF [10,11]. Since the transfer of the ChR2 gene into RGCs was not regulated according to RGC type in these studies, it is possible that all RGC types became photosensitive. Thus, RGC-derived signals must be reinterpreted by the brain in order to organize effective vision. Transgenic rats that express ChR2 in RGCs provide a useful experimental model with which to evaluate quantitatively the visual function of an animal in which RGCs are made photosensitive by the expression of ChR2.

The Thy-1.2 antigen is a glycoprotein found on the cell surface of a variety of cell types [12,13]. Rat Thy-1.2 antigen has been found to be abundant in the brain and thymus [14,15]. In the retina, the Thy-1.2 antigen is recognized to be a marker specific to RGCs [16,17]. Thus, the Thy-1.2 promoter is an effective regulator of a gene that is expressed exclusively in the RGCs [18,19,20]. In the present study, we generated transgenic rats in which the ChR2 transgene was driven by the Thy-1.2 promoter. One of them, line 4 (W-TChR2V4), expressed ChR2 specifically

in the RGCs of the entire retina. We found that contrast sensitivities of optomotor responses in W-TChR2V4 rats were equivalent to wild-type rats, even when native photoreceptor cells were degenerated by continuous light exposure. However, contrast sensitivities at low spatial frequencies were enhanced after photoreceptor cell degeneration. This suggests that the visual signals derived from the ChR2-expressing RGCs are reinterpreted to form behavior-related vision.

Results

Generation of Transgenic Rats

The Thy-1.2 vector derived from a 6.5-kb fragment of the murine Thy-1.2 gene has been reported to promote gene expression in RGCs and in neurons in the brain [21] (Fig. 1A). We analyzed the genomic insertion of a ChR2V cDNA fragment by performing polymerase chain reaction (PCR) on tail DNA and subsequently detected a PCR product of 324 bp in eight founder rats (Fig. 1B). We termed these transgene positive lines "Wistar-Thy-1.2 promoter-Channelrhodopsin 2-Venus rats" (W-TChR2V). Among these 8 lines (W-TChR2V1-8), 6 lines, which were capable of reproduction and transgenerational propagation of the transgene, were evaluated further for expression of the ChR2V protein in the retina.

Under fluorescence microscopy, ChR2V was shown to be expressed in the retina of the heterozygous rat (ChR2V +/−) in four of six lines of transgenic rats: W-TChR2V1, W-TChR2V4, W-TChR2V5, and W-TChR2V7 (Fig. 2A–D). As shown in Fig. 2, ChR2V expression was extensively observed in the flat-mounted retina. Vertical sections indicated that cells expressing ChR2V were distributed differently in each transgenic line. In the case of W-TChR2V1, the "Venus" marker fluorescence (see Methods section) was observed in the RGC layer (GCL), inner plexiform layer (IPL), and outer plexiform layer (OPL). The W-TChR2V4 strain showed ChR2V expression in the GCL and IPL. In addition to expression in these layers, strains W-TChR2V5 and W-TChR2V7 showed intense fluorescence in the inner nuclear layer (INL). When the flat-mounted retina of the W-TChR2V4 rat was vertically examined using the z-axis scanning mode of the microscope, the Venus fluorescence was colocalized with Fluorogold, which retrogradely labeled the RGCs (Fig. 2E).

Direct Photoactivation of ChR2V-Expressing RGCs

We expected that the ChR2V-expressing RGCs in the W-TChR2V4 rat retina would be sensitive to light. To test this hypothesis, we investigated the light-evoked responses of ChR2V-expressing RGCs, while all the synaptic inputs derived from the photoreceptor cells were pharmacologically blocked by 1 mM kynurenic acid, a nonselective glutamate receptor blocker. In a ChR2V-expressing RGC placed under whole-cell voltage clamp at −60 mV (Fig. 3A), a blue light-emitting diode (LED) light pulse evoked an inward current whose amplitude was dependent on the light power density (Fig. 3B). The light-evoked current has similarities to a ChR2 photocurrent [6], i.e. rapid onset without detectable latency, peak-and-plateau biphasic kinetics, and a rapid offset. The onset time constant was dependent on the light power density, but 4–9 ms in this case. The offset time constant was less dependent on the light power density and was 15–18 ms. Under current-clamp configuration, membrane potential was depolarized by an LED light pulse with an undetectable delay and was accompanied by action potentials (Fig. 3C). Action potentials were evoked by a 100-ms LED pulse with a power density as low as $3.7 \pm 2.3\ \mu W/mm^2$ ($n = 14$). We found that the action potential could also be evoked by an LED light pulse as short as 10 ms (Fig. 3D).

Degeneration of Photoreceptor Cells

There were 11–12 rows of photoreceptor nuclei in the outer nuclear layer (ONL) of the transgenic rats; this is a number usually

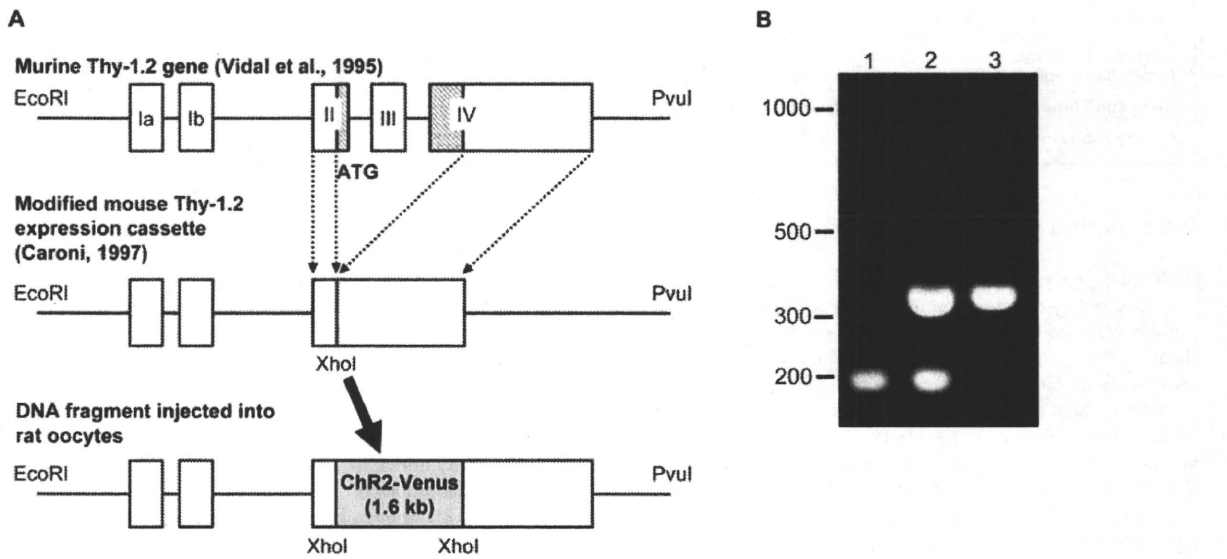

Figure 1. Generation of Thy-1.2 ChR2V transgenic rat. Schematic drawing of DNA fragment injected into rat oocytes. (A) The cDNA coding channelrhodopsin-2 (ChR2) tagged with Venus was inserted at XhoI site of the modified mouse Thy-1.2 expression cassette. A linearized DNA fragment (7.5 kb) prepared by digestion with EcoRI and PvuI restriction enzymes was injected into rat oocytes. (B) Examples of PCR analysis of genomic DNA from transgenic founder rats injected with the transgene shown in A. Genomic DNAs from the injected DNA fragment (lane 1), a transgenic founder (lane 2) and a non transgenic founder (lane 3) were amplified by PCR. DNA bands at 173 bp and 324 bp correspond to amplified DNA fragments for the transgene (ChR2-Venus, ChR2V) and the T cell receptor gene as an internal control, respectively.
doi:10.1371/journal.pone.0007679.g001

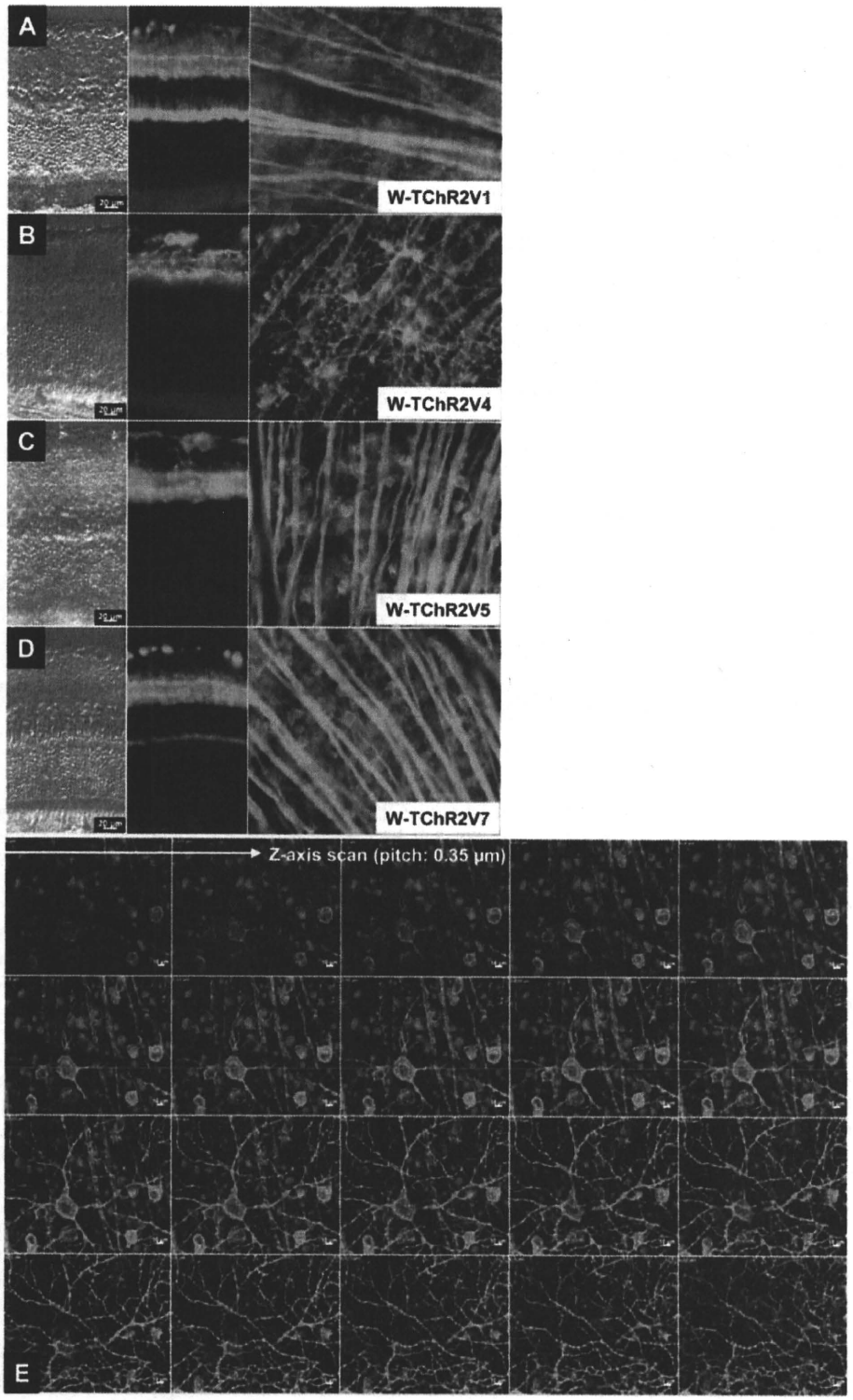

Figure 2. Microphotographs showing ChR2V expression in the inner retinal layers of each transgenic line. (A–D) The retinal organization of each transgenic line (A, W-TChR2V1; B, W-TChR2V4; C, W-TChR2V5; D, W-TChR2V7) showed normal features in the Nomarskii images (left). Fluorescence microphotography revealed various expression patterns in retinal slices (middle) and flat-mounted retinas (right). (E) Z-axis scan (pitch: 0.35 μm) images collected from a flat-mounted retina of a ChR2V+/− rat (line W-TChR2V4) showed that the ChR2V fluorescence (green) was coexpressed with fluorogold transported retrograde from the superior colliculus (blue).
doi:10.1371/journal.pone.0007679.g002

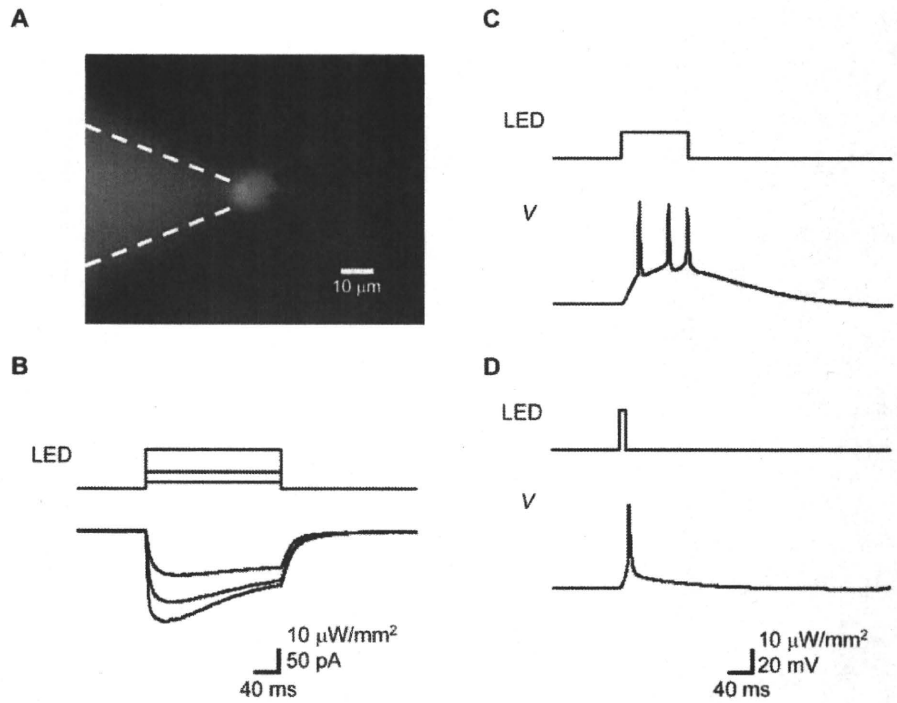

Figure 3. Direct photoactivation of ChR2V-expressing RGCs. (A) The blue light-emitting diode (LED)-evoked membrane currents and potentials were recorded under whole-cell recording from one of the ChR2V-expressing RGCs. (B) The photocurrents and their dependency in the LED power density. (C–D) The membrane potential responses of a ChR2V-expressing RGC to LED pulses of 100-ms (C) or 10-ms (D) duration.
doi:10.1371/journal.pone.0007679.g003

observed in rodents without retinal degeneration [22] and indicates that the ectopic expression of ChR2V did not affect retinal structure (Fig. 4A, B). After continuous toxic light exposure, the cells in the ONL were almost absent in both the superior and inferior retinas from both the ChR2V−/− (Fig. 4C) and ChR2V+/− rats (Fig. 4D). The disappearance of the ONL was also noted under low magnification in a slice of the whole retina (Fig. 4E, F). Even after photoreceptor degeneration, the ChR2-expressing RGCs remained in the ChR2V+/− rats (Fig. 4G).

When the visual signals generated by the photoreceptor cells are transmitted to inner retinal neurons, the associated change in the electric field of the retina is evaluated as the electroretinogram (ERG) response. Typical waveforms of ERGs were observed in either the ChR2V−/− or the ChR2V+/− rats (Fig. 5A; upper). We found that the a- and b-wave ERG amplitude was small in the ChR2V+/− rats when evoked by the blue LED light. Both a- and b- wave amplitudes were significantly higher in ChR2V−/− than in ChR2V+/− rats (Fig. 5B). With regard to the latency of the a-wave, no detectable difference was observed between the ChR2V−/− and ChR2V+/− rats (Fig. 5B). On the other hand, the ERG response of the ChR2V+/− rats was quantitatively similar to that of the ChR2V−/− rats when evoked by the red LED light (Fig. 5A; lower, C). Since the blue LED light, but not the red LED light, was absorbed by both the ChR2 and Venus protein, photon density of the blue LED light may have been reduced before reaching the photoreceptor cells.

After exposing the rats to 3000-lux light continuously for 7 days, the ERG responses were evaluated with the blue LED and red LED (Fig. 5D). The ERG responses were almost negligible with either the blue or the red LED at intensities of 10–1000 lux. Amplitudes of the a- or b-wave were markedly decreased in both the ChR2v −/− and +/− rats, which indicated that retinal function had been damaged by the continuous light exposure (Fig. 5E). This ERG reduction was adopted as a criterion of photoreceptor degeneration in the following experiments.

Visually Evoked Potentials

In a normal eye, the visual signal is first received by the photoreceptor cells, transmitted and integrated in the retinal neuronal network, projected to the brain by the RGCs, eventually arriving at the visual cortex through synapses in the lateral geniculate nucleus. This signaling chain is evaluated as a whole by the visually evoked potential (VEP), a visual cortical response triggered by a short light pulse. Figure 6A shows sample rat VEPs before inducing photoreceptor degeneration. VEPs were recorded in both the ChR2V−/− and ChR2V+/− rats. When the VEPs were evoked by the weak blue LED light, those of the ChR2V+/− rats were similar to those of the ChR2V−/− rats. However, with the strong blue LED light (>240 lux), the VEP of the ChR2V+/− rat was larger in amplitude and shorter in latency than that of the ChR2V−/− rat (Fig. 6B). This suggests that the strong blue LED light induces the ChR2V-expressing RGCs to fire directly, without mediation by photoreceptor cells.

On the other hand, when VEPs were evoked by the red LED light, those of the ChR2V+/− rats were similar to those of the ChR2V−/− rats in both amplitude and time course (Fig. 6A). No significant differences were present in the VEP amplitude-stimulus intensity relationships, and the latency-stimulus intensity relationship of the ChR2V+/− rats was also identical to that of the ChR2−/− rats (Fig. 6C).

The VEPs were then recorded after exposing the rats to 3000 lux light continuously for 7 days. After subsequent

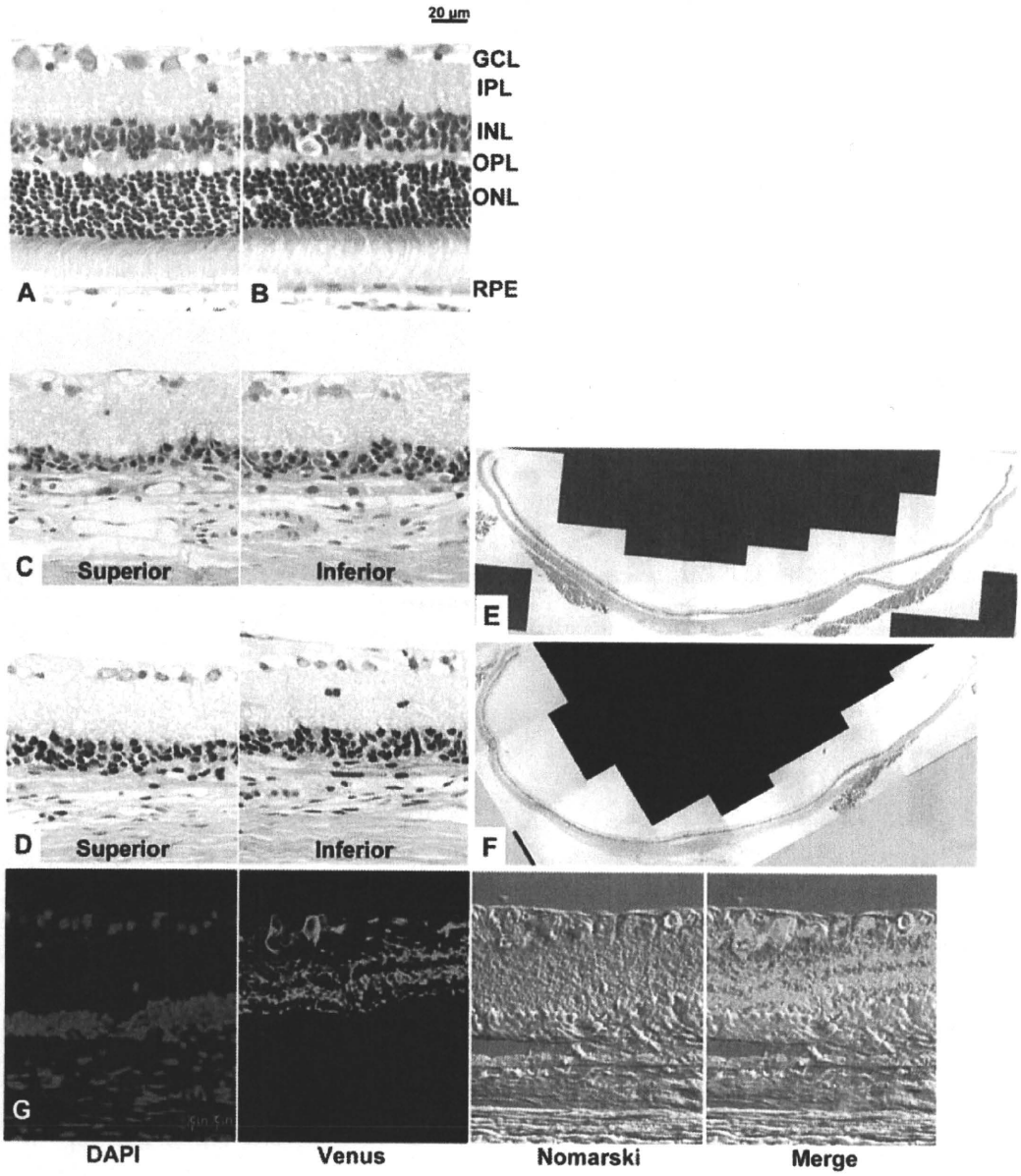

Figure 4. Morphological evidences of the photoreceptor degeneration in either ChR2V−/− or ChR2V+/− rats. (A, B) Normal retinal architecture was observed in each rat before photoreceptor degeneration. (C, D) After continuous light exposure (3000 lux for 7 days). Sections are from the superior and inferior regions at a distance of 0.24 mm from the optic nerve. Note the absence of the outer nuclear layer. (E, F)The severe degeneration extended to the whole retina. (G)Cryo-section of a retina from a ChR2V+/− rat. ChR2V expression was observed in the inner layer. Abbreviations: GCL, ganglion cell layer; IPL, inner plexiform layer; INL, inner nuclear layer; OPL, outer plexiform layer; ONL, outer nuclear layer; RPE, retinal pigment epithelium.
doi:10.1371/journal.pone.0007679.g004

degeneration of most of the photoreceptor cells, the VEPs resulting from either blue or red light were almost negligible in the ChR2V−/− rats (Fig. 7A). In contrast, in the ChR2V+/− rats, the VEPs evoked by the blue LED light clearly remained, even after photoreceptor degeneration (Fig. 7B); however, the VEPs evoked by the red LED were negligible (Fig. 7C). As shown in the amplitude-stimulus intensity relationship (Fig. 7B), the remaining VEPs were induced only by strong blue LED light (>240 lux). These VEPs were again characterized by shortened latency periods.

Optomotor Responses of the Rats

The spatial vision of an animal was quantified by its optomotor response. When a drum is rotated around an animal with printed visual stimuli on the inside wall, the animal tracks the stimulus by turning its head [23]. In our virtual optomotor system, a stimulus of blue stripes over a black background was produced according to a sine wave function with variable amplitude and frequency (Fig. 8A). With a given spatial frequency, the rat tracked the objects if the brightness-darkness contrast was high. However, the rat's response became

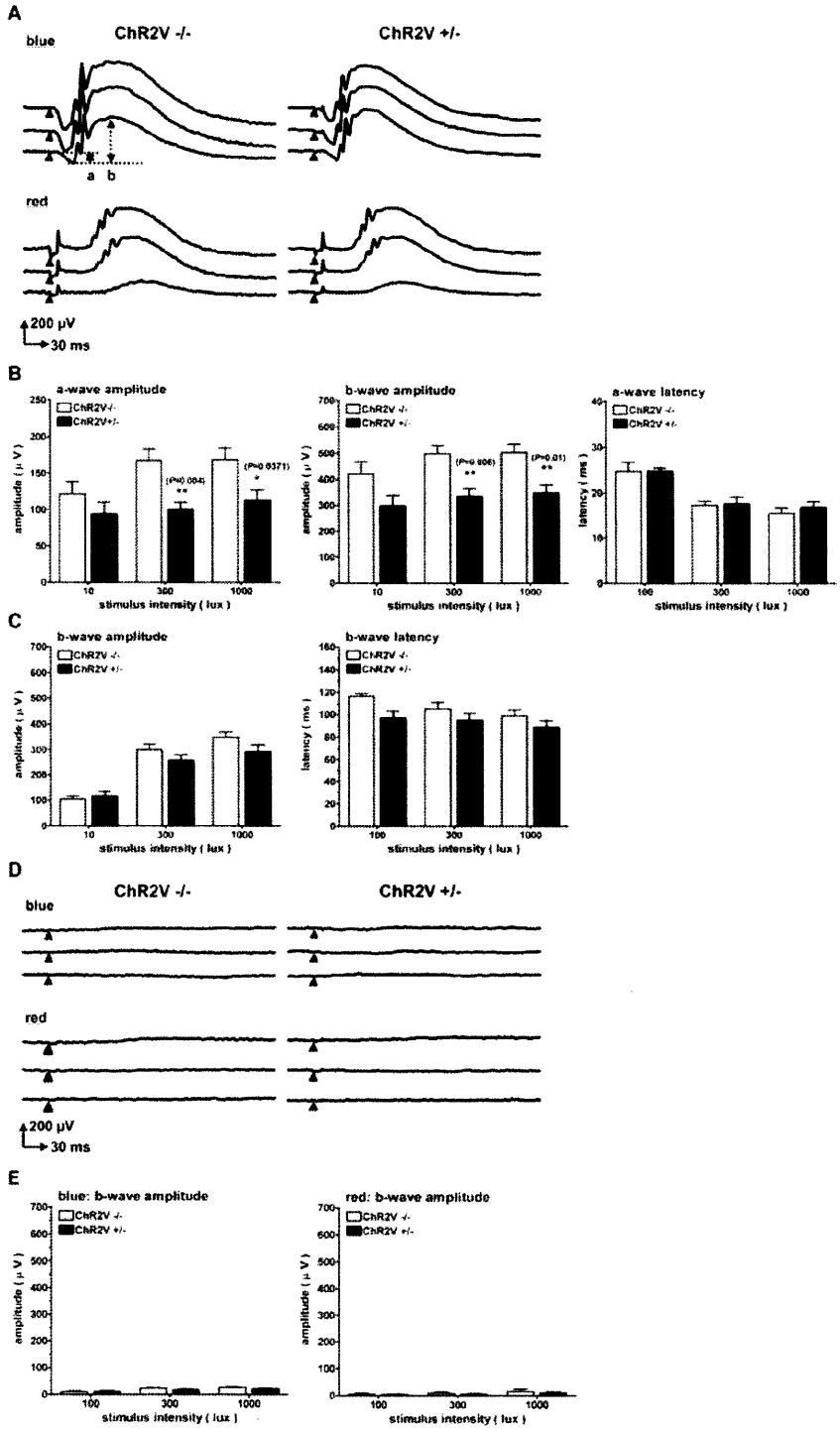

Figure 5. Electrophysiological evidence of photoreceptor degeneration. (A) Typical waveforms of electroretinogram (ERG) responses evoked by either blue or red light-emitting diode (LED) flash (duration: 10 ms; light intensity: 1000, 300, and 100 lux, top to bottom). (B)The ERG amplitudes (left, a-wave; middle, b-wave) and the latency of the a-wave (right) in response to the blue LED flash. Note that both amplitudes were significantly diminished in the ChR2V+/− rats compared to the ChR2V−/− rats without any differences in a-wave latency. (C) The b-wave amplitudes (left) and the latency (right) in response to the red LED flash. (D)Typical ERG waveforms evoked by either blue (upper traces) or red (lower traces) LED flash in the ChR2V−/− (left) and +/− (right) rats after continuous light (3000 lux) exposure for 7 days. (E)The b-wave amplitudes recorded from the rats after continuous light exposure. Error bars represent standard deviation (n = 8, **: $P<0.01$, unpaired t-test).
doi:10.1371/journal.pone.0007679.g005

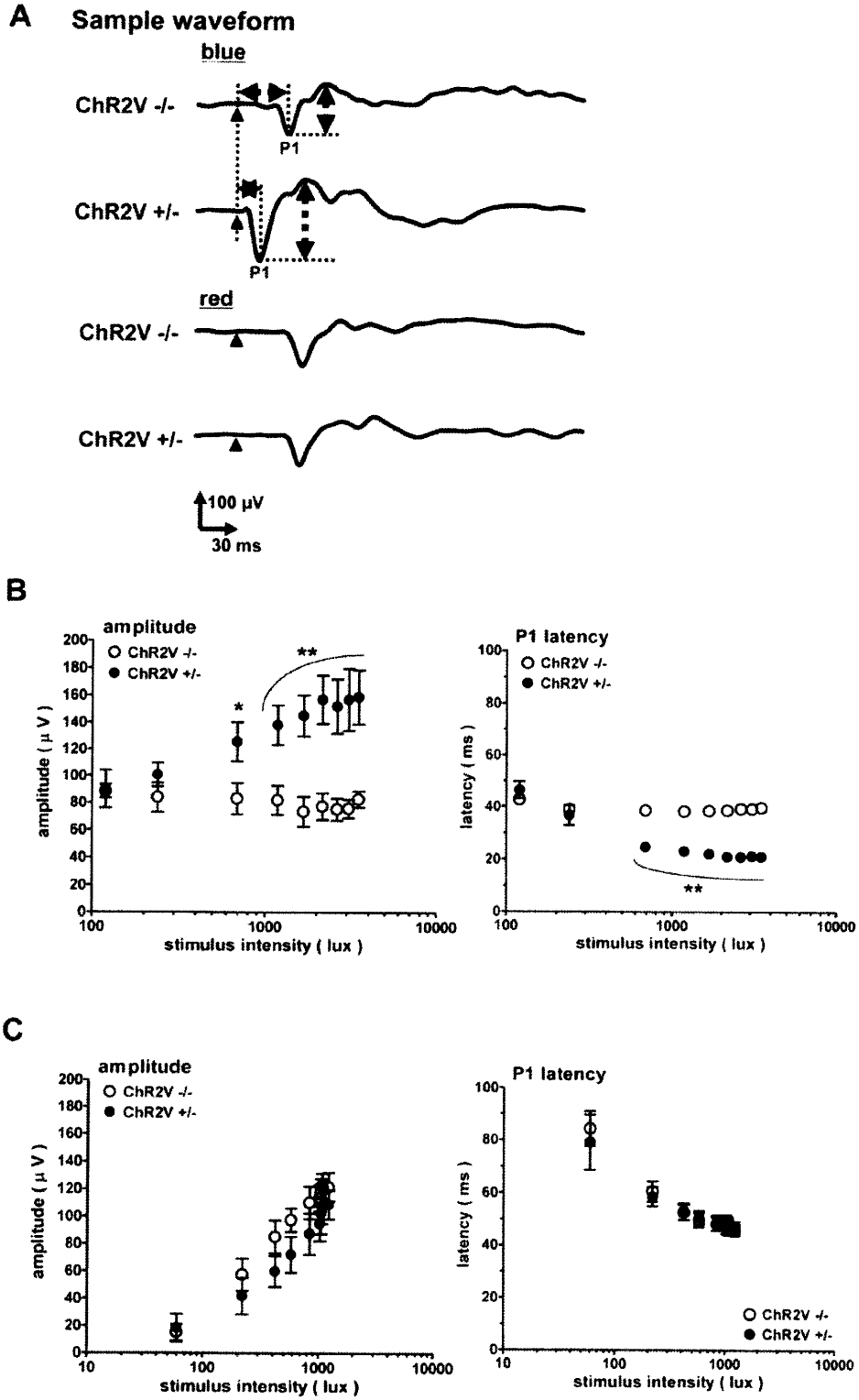

Figure 6. The visually evoked potentials recorded from either the ChR2V−/− or ChR2V+/− rats before photoreceptor degeneration. (A)Sample waveforms evoked by the blue or red LED flash. (B) The amplitude- (left) and the latency- (right) stimulus intensity relationships of VEPs evoked by the blue LED flash. (C) Similar to (A), but the responses are to the red LED flashes. Error bars represent standard deviation (n = 8, *: P = 0.04, **: P<0.01, unpaired t-test).
doi:10.1371/journal.pone.0007679.g006